

# Geometrical Realization of Beutler-Fano formulas appearing in eigenphase shifts and time delays in multichannel scattering

Chun-Woo Lee

*Department of Chemistry, Ajou University, 5 Wonchun Dong, Suwon 442-749, KOREA*

Recently, we showed that eigenphase shifts and eigentime delays near a resonance for a system of one discrete state and two continua are functionals of the Beutler-Fano formula using appropriate dimensionless energy units and line profile indices and identified parameters responsible for the avoided crossing of eigenphase shifts and eigentime delays and also parameters responsible for the eigentime delays due to a change in frame transformation.

In this paper, the geometrical realization of the Beutler-Fano formulas is considered in the real three-dimensional Liouville space spanned by the Pauli matrices  $\sigma_x$ ,  $\sigma_y$ ,  $\sigma_z$  which are orthogonal in the sense that  $\text{Tr}(\sigma_i\sigma_j) = 2\delta_{ij}$ , where dynamic operators are vectors. Vectors corresponding to the background  $S^0$  matrix,  $S$  matrix, and the time delay matrix  $Q$  form a spherical triangle whose vertex and edge angles are parameters pertaining to the frame transformations among eigenchannels of  $S^0$ ,  $S$ ,  $Q$  and eigenphase shifts of  $S^0$  and  $S$  and the phase shift due to a resonance scattering. The cotangent laws of the spherical triangle yield Beutler-Fano resonance formulas appearing in eigenphase shifts and time delays. Duality holding for the spherical triangle explains the symmetry observed in the relations among parameters and provides a systematic way of defining conjugate dynamic parameters. The spherical triangle also shows the rule of combining the channel-channel couplings in the background scattering with the resonant interaction to give the avoided crossing interactions in the curves of eigenphase shifts as functions of energy.

The theory developed in the previous and present papers is applied to the vibrational predissociation of triatomic van der Waals molecules.

03.65.Nk, 11.80.Gw, 33.80Gj, 34.10.x

## I. INTRODUCTION

Eigenphase shifts  $\delta_i$  ( $i = 1, 2, \dots, n$ ) of the  $S$  matrix, defined as

$$S = Ue^{2i\delta}\bar{U} \quad (1)$$

have been utilized as a tool for analyzing the resonances [1,2]. Eigenphase shifts and the corresponding eigenchannels are also extensively used in various forms in multichannel quantum-defect theory (MQDT) which is one of the most powerful theories of resonance [3]. In MQDT, the first derivatives of eigenphase shifts as functions of energy are used for various purposes [4]. The Lu-Fano plot is essentially a plot of the energy derivative of an eigenphase shift [3]. The first derivative of an eigenphase shift as a function of energy, called “a partial delay time”, has also studied as a relevant quantity to time delays in various fields [5].

In spite of their wide use, studies of the behaviors of eigenphase shifts and their energy derivatives in the neighborhood of a resonance have not been done extensively, comparing to the studies of photo-fragmentation cross sections and  $S$  matrix itself. Eigenphase shifts in the multichannel system are known to show complicated behaviors near a resonance due to the avoided crossing between curves of eigenphase shifts along the energy [1,6]. In the previous work, detailed studies of the behaviors of eigenphase shifts and times delayed by collision were done for the system of one discrete state and two continua [7]. Comparing to the system of one discrete state and one continuum, the newly added one more continuum brings about the new phenomena of the avoided crossing between curves of eigenphase shifts and eigentimes delayed and of times delayed due to the change in frame transformation along the energy besides the resonance behavior. Thus the system of one discrete state and two continua provides a prototypical system for the study of two effects on the resonance phenomena, avoid crossings between eigenphase shifts and eigentimes delayed as one effect and the change in frame transformation as another one.

Previous work showed that eigenphase shifts and eigentimes delayed due to the avoided crossing interaction and eigentimes delayed due to the change in frame transformation are functionals of the Beutler-Fano formula using the appropriate dimensionless energy units and line profile indices [7]. Parameters representing the avoided crossing of eigenphase shifts and eigentime delays were identified. Parameters representing the eigentime delays due to a change in frame transformation were shown to be described by the same parameters. With the help of new parameters, the

rotation angle  $\theta$  and rotation axis  $\hat{n}$  for the  $S$  matrix  $\exp[i(a + \theta\sigma \cdot \hat{n})]$  were identified. The time delay matrix  $Q$  was shown to be given as  $Q = \frac{1}{2}\tau_r(\mathbf{1} + \mathbf{P}_a \cdot \boldsymbol{\sigma} + \mathbf{P}_f \cdot \boldsymbol{\sigma})$  where the first term is the time delay due to the resonance, the second term is the one due to the avoided crossing interaction and the last term is the one due to the change in frame transformation.

Though previous work found that behaviors of eigenphase shifts and eigentime delays as functions of energy follow Beutler-Fano's formula, it could not explain why they follow Beutler-Fano's formula. Since the system considered in the previous work is essentially two channel system (with one more discrete state), an analogy with the spin system was made and utilized but not fully exploited. One of the main purpose of the present paper is to exploit the analogy further. Especially, the homomorphism of the spin model with the three-dimensional rotation will be fully exploited to construct geometric structures made up of dynamical parameters for eigenphase shifts and eigentime delays and thus to derive the Beutler-Fano's formula geometrically. The geometrical realization clarifies the ambiguities in relations and unexplained meanings of dynamic parameters at the previous work since the geometric constructions appeal to our intuition and are thus easy to understand and provides means of viewing complicated relations in a simple way. This clarification of complicated dynamic relations through the geometrical realization is another main goal of this paper.

Section II summarizes the previous results. Section III modifies the previous results a little suitable for the geometrical realization. Section IV gives a geometrical realization of the previous results. Section V connects the geometrical relations with the dynamical ones. Section VI applies the theory developed in Ref. [7] and the present paper to the vibrational predissociation of triatomic van der Waals molecules. Section VII summarizes and discusses the results.

## II. SUMMARY OF THE PREVIOUS RESULT

Ref. [7] examined eigenphase shifts and eigentime delays in the neighborhood of an isolated resonance for the system of one discrete state and two continua as a prototypical system for the study of the combined effects of the resonance and the indirect continuum-continuum interaction via a discrete state. The  $S$  matrix for an isolated resonance system is well known and, if the background  $S^0$  matrix is described by its eigenphase shifts  $\delta^0$  as  $S^0 = U^0 e^{-2i\delta^0} \tilde{U}^0$ , takes the form [8]

$$S_{jk} = \sum_{l,m} U_{jl}^0 e^{-i\delta_l^0} \left( \delta_{lm} + i \frac{\sqrt{\Gamma_l \Gamma_m}}{E - E_0 - i\Gamma/2} \right) e^{-i\delta_m^0} \tilde{U}_{mk}^0, \quad (2)$$

where  $\Gamma_l$ ,  $\Gamma$ ,  $E_0$  are the partial decay width of a resonance state into the  $l$ th background eigenchannel [9], the total decay width  $\sum_l \Gamma_l$ , and the resonance energy, respectively. Eq. (2) is for the incoming wave boundary condition. The formula for the outgoing wave boundary condition differs from Eq. (2) in that  $i$  is replaced by  $-i$ .

By diagonalizing Eq. (2), eigenphase shifts  $\delta$  of the  $S$  matrix ( $=Ue^{-2i\delta}\tilde{U}$ ) for the system of one discrete state and two continua were obtained as

$$2\delta_{\pm}(E) = \sum_i \delta_i^0 + \delta_r(E) \pm \delta_a(E), \quad (3)$$

where  $\delta_r(E)$  is the well-known resonance phase shift due to the modification of the scattering wave by the quasi-bound state and given by  $-\arctan(1/\epsilon_r)$  and  $\delta_a(E)$  is the one due to the modification of the scattering wave by the other wave through the indirect interaction via the quasi-bound state and was found to be given as a functional of the Beutler-Fano formula [10]

$$\cot \delta_a(E) = -\cot \Delta_{12}^0 \frac{\epsilon_a - q_a}{(1 + \epsilon_a^2)^{1/2}}, \quad (4)$$

in the dimensionless energy scale defined by

$$\epsilon_a \equiv \frac{2(E - E_a)}{\Gamma_a}, \quad (5)$$

where  $\Gamma_a = 2\sqrt{\Gamma_1 \Gamma_2}/|\sin \Delta_{12}^0|$  and  $E_a = E_0 + \frac{\Delta\Gamma}{2} \cot \Delta_{12}^0$  ( $\Delta\Gamma = \Gamma_1 - \Gamma_2$ ,  $\Delta_{12}^0 = \delta_1^0 - \delta_2^0$ ). Its form as a functional of the Beutler-Fano formula can be shown more explicitly by using the Beutler-Fano function

$$f_{\text{BF}}(\epsilon, q) \equiv \frac{(\epsilon - q)^2}{1 + \epsilon^2}, \quad (6)$$

as

$$\cot \delta_a(E) = \begin{cases} \cot \Delta_{12}^0 \sqrt{f_{\text{BF}}(\epsilon_a, q_a)} & \text{when } \epsilon_a < q_a \\ -\cot \Delta_{12}^0 \sqrt{f_{\text{BF}}(\epsilon_a, q_a)} & \text{when } \epsilon_a \geq q_a. \end{cases} \quad (7)$$

The line profile index  $q_a$  of the curve of  $\delta_a(E)$  is given by

$$q_a = -\frac{\Delta\Gamma}{2\sqrt{\Gamma_1\Gamma_2} \cos \Delta_{12}^0}. \quad (8)$$

When  $\epsilon_a = q_a$ ,  $\delta_a = \pi/2$  and the difference in abscissas of two eigenphase shift curves is  $\pi/2$  which is the largest separation of two curves when  $\delta_a$  is defined up to  $\pi$ . Therefore, the line profile index  $q_a$  also stands for the energy of maximal avoidance of eigenphase shifts. Eq. (2) shows that the eigenphase sum  $\delta_\Sigma$  is given by  $\delta_\Sigma = \sum_i \delta_i^0 + \delta_r = \delta_\Sigma^0 + \delta_r$ , in conformity with Hazi's formula [11].

Let us define  $\mathcal{S}$  by  $S = U^0 \tilde{S} U^0$ . Let  $\mathcal{S}$  be diagonalized by the  $V$  matrix composed of eigenvectors corresponding to  $\delta_+$  and  $\delta_-$  as  $V = (v_+, v_-)$ . The  $V$  matrix was obtained as

$$V = \begin{pmatrix} \cos \frac{\theta_a}{2} & -\sin \frac{\theta_a}{2} \\ \sin \frac{\theta_a}{2} & \cos \frac{\theta_a}{2} \end{pmatrix}, \quad (9)$$

where  $\theta_a$  is defined by

$$\cos \theta_a = -\frac{\epsilon_a}{\sqrt{1 + \epsilon_a^2}}, \quad \sin \theta_a = \frac{1}{\sqrt{1 + \epsilon_a^2}}. \quad (10)$$

Eigenvectors are independent of  $q_a$ . They depend only on  $\epsilon_a$ . As  $\epsilon_a$  varies from  $-\infty$  through zero to  $\infty$ ,  $\theta_a$  varies from zero through  $\pi/2$  to  $\pi$  and  $v_+$  varies from  $\begin{pmatrix} 1 \\ 0 \end{pmatrix}$  through  $\frac{1}{\sqrt{2}} \begin{pmatrix} 1 \\ 1 \end{pmatrix}$  to  $\begin{pmatrix} 0 \\ 1 \end{pmatrix}$ . Thus, at  $\epsilon_a = 0$  or at  $E = E_0 + \frac{\Delta\Gamma}{2} \cot \Delta_{12}^0$ , two background eigenchannels are mixed equally. For this reason  $\epsilon_a = 0$  is regarded as the avoided crossing point energy. This energy does not coincide with the energy  $\epsilon_a = q_a$  where two eigenphase shift curves are separated most. Let  $U = U^0 V$ , then  $U$  diagonalizes the  $S$  matrix, that is, the transform  $\tilde{U} S U$  is the diagonal matrix  $e^{-2i\delta}$ . The  $U$  matrix is obtained from the  $V$  matrix by replacing  $\theta_a$  with  $\theta'_a = \theta_a + \theta^0$ , where  $\theta^0$  parametrizes  $U^0$  matrix as

$$U^0 = \begin{pmatrix} \cos \frac{\theta^0}{2} & -\sin \frac{\theta^0}{2} \\ \sin \frac{\theta^0}{2} & \cos \frac{\theta^0}{2} \end{pmatrix}, \quad (11)$$

With the new parameters and Pauli's spin matrices, the  $S$  matrix was found to be expressible as

$$S = e^{-i(\delta_\Sigma \mathbf{1} + \delta_a \boldsymbol{\sigma} \cdot \hat{n}'_a)}, \quad (12)$$

where

$$\hat{n}'_a = \hat{z} \cos \theta'_a + \hat{x} \sin \theta'_a. \quad (13)$$

Smith's time delay matrix  $Q (=i\hbar S^\dagger \frac{dS}{dE}$  [12,13]) can be easily obtained by substituting Eq. (12) into its definition and was found to consist of three terms

$$Q = \frac{1}{2}(\mathbf{1}\tau_r + \boldsymbol{\sigma} \cdot \hat{n}'_a \tau_a + \boldsymbol{\sigma} \cdot \hat{n}'_f \tau_f), \quad (14)$$

one due to the resonance, one due to the avoided crossing interaction, and one due to the change in frame transformation as a function of energy, where

$$\hat{n}'_f = \hat{y} \times \hat{n}'_a \cos \delta_a - \hat{y} \sin \delta_a, \quad (15)$$

and is orthogonal to  $\hat{n}'_a$ .

The time delay due to the resonance takes a symmetric Lorentzian form

$$\tau_r(E) = 2\hbar \frac{d\delta_r(E)}{dE} = \frac{4\hbar}{\Gamma} \frac{1}{1 + \epsilon_r^2}, \quad (16)$$

and the time delay due to the avoided crossing was found to take a form of a functional of the Beutler-Fano formula

$$\tau_a(E) = -\tau_r(E) \frac{\epsilon_r - q_\tau}{\sqrt{(\epsilon_r - q_\tau)^2 + r^2(1 + \epsilon_r^2)}} \quad (17)$$

$$= \begin{cases} \tau_r(E) \sqrt{\frac{f_{\text{BF}}(\epsilon_r, q_\tau)}{f_{\text{BF}}(\epsilon_r, q_\tau) + r^2}} & \text{when } \epsilon_r \leq q_\tau \\ -\tau_r(E) \sqrt{\frac{f_{\text{BF}}(\epsilon_r, q_\tau)}{f_{\text{BF}}(\epsilon_r, q_\tau) + r^2}} & \text{when } \epsilon_r > q_\tau, \end{cases} \quad (18)$$

where parameters  $r$  and  $q_\tau$  are defined by

$$r \equiv \frac{\sqrt{\Gamma^2 - \Delta\Gamma^2}}{\Delta\Gamma}, \quad (19)$$

$$q_\tau \equiv \frac{\Gamma}{\Delta\Gamma} \cot \Delta_{12}^0, \quad (20)$$

The asymmetry of  $\tau_a$  as a function of energy is brought about by the nonzero value of  $q_\tau$  which is proportional to the shift of the avoided crossing point energy from the resonance one. Thus the asymmetry of  $\tau_a$  is caused by the mismatch in the positions of the avoided crossing point and resonance energies. The time delay due to a change in frame transformation was found to take the following form [14]

$$\tau_f(E) = \tau_r(E) \frac{|r|}{\sqrt{f_{\text{BF}}(\epsilon_r, q_\tau) + r^2}}. \quad (21)$$

Because of the last term of Eq. (14), eigenfunctions of the  $Q$  matrix are different from those of the  $S$  matrix. The eigentime delay sum, which is equal to  $\sum_i Q_{ii} = \text{Tr}Q$ , is obtained as

$$\sum_i Q_{ii} = \text{Tr}Q = \tau_r, \quad (22)$$

since  $\text{Tr}\sigma = 0$ . The consideration of the transforms  $\tilde{U}^0 S U^0$  and  $\tilde{U}^0 Q U^0$ , which will be denoted as  $\mathcal{S}$  and  $\mathcal{Q}$ , will be proved to be more convenient later for the geometric consideration. The transforms  $\mathcal{S}$  and  $\mathcal{Q}$  are the scattering and time delay matrices with the background eigenchannel wavefunctions as a basis instead of the asymptotic channel wavefunctions [9], whose forms in terms of the new parameters and Pauli's spin matrices are the same as those of  $S$  and  $Q$  but with vectors  $\hat{n}_a$  and  $\hat{n}_f$  which are obtained from  $\hat{n}'_a$  and  $\hat{n}'_f$  by replacing  $\theta'_a$  with  $\theta_a$ .

The connection of the time delay matrix  $Q$  with the time delay experienced by a wave packet was first considered by Eisenbud [15] and extended by others [16]. According to their work,  $Q_{ii}$  is the average time delay experienced by a wave packet injected in the  $i$ th channel. Here, the average time delays due to the avoided crossing interaction are given by  $\tau_a \cos \theta'_a/2$  and  $-\tau_a \cos \theta'_a/2$ . Similarly, the average time delays due to the change in frame transformation are  $-\tau_f \sin \theta'_a \cos \delta_a/2$  and  $\tau_f \sin \theta'_a \cos \delta_a/2$ . Time delays due to the avoided crossing interaction and the change in frame transformation are out of phase by  $\pi/2$ . Overall,  $Q_{11} = \frac{1}{2}(\tau_r + \tau_a \cos \theta'_a - \tau_f \sin \theta'_a \cos \delta_a)$  and  $Q_{22} = \frac{1}{2}(\tau_r - \tau_a \cos \theta'_a + \tau_f \sin \theta'_a \cos \delta_a)$ .

In analogy with the spin  $\frac{1}{2}$  system, the time delay matrix  $Q$  was expressed in terms of polarization vectors and the Pauli spin matrices as

$$Q = \frac{1}{2} \tau_r (\mathbf{1} + \mathbf{P}_a \cdot \boldsymbol{\sigma} + \mathbf{P}_f \cdot \boldsymbol{\sigma}), \quad (23)$$

where polarization vectors are defined by

$$\mathbf{P}_a = \frac{\tau_a}{\tau_r} \hat{n}'_a, \quad \mathbf{P}_f = \frac{\tau_f}{\tau_r} \hat{n}'_f. \quad (24)$$

Like the spin  $\frac{1}{2}$  system, it was found that the absolute values of  $\mathbf{P}_a$  and  $\mathbf{P}_f$  are restricted to  $0 \leq |\mathbf{P}_a| \leq 1$  and  $0 \leq |\mathbf{P}_f| \leq 1$ . In the present case a complete depolarization means that eigentime delays are the same regardless of eigenchannels, while a complete polarization means that eigentime delays are 0 for one eigenchannel and  $\tau_r(E)$  for another eigenchannel. Eigenvectors for eigentime delays due to an avoided crossing interaction and due to a change in frame transformation are orthogonal to each other and contribute to the total eigentime delays as  $\sqrt{\tau_a^2 + \tau_f^2} = \tau_r \sqrt{|\mathbf{P}_a|^2 + |\mathbf{P}_f|^2}$ . It was found that

$$|\mathbf{P}_a|^2 + |\mathbf{P}_f|^2 = 1. \quad (25)$$

Since  $\mathbf{P}_a$  and  $\mathbf{P}_f$  are mutually orthogonal and  $|\mathbf{P}_a|^2 + |\mathbf{P}_f|^2 = 1$ , we can define a vector  $\mathbf{P}_t = \mathbf{P}_a + \mathbf{P}_f$ , whose magnitude is unity. Its formula may be obtained straightforwardly but hardly used. Instead, the formula of its transform  $\mathcal{P}_t = \tilde{U}^0 \mathbf{P}_t U^0$  is exclusively used, which is much simpler and given as

$$\mathcal{P}_t \equiv \hat{n}_t = \left( \cos \Delta_{12}^0 \frac{\sqrt{\Gamma^2 - \Delta\Gamma^2}}{\Gamma}, -\sin \Delta_{12}^0 \frac{\sqrt{\Gamma^2 - \Delta\Gamma^2}}{\Gamma}, \frac{\Delta\Gamma}{\Gamma} \right). \quad (26)$$

The transform  $\mathcal{P}_t$  is the total polarization vector for the time delay matrix  $Q (= \tilde{U}^0 Q U^0)$  with background eigenchannels used as the basis. The similar transforms  $\mathcal{P}_a$  and  $\mathcal{P}_f$  of  $\mathbf{P}_a$  and  $\mathbf{P}_f$  will be used later and satisfy the same relations  $\mathcal{P}_t = \mathcal{P}_a + \mathcal{P}_f$  and

$$|\mathcal{P}_a|^2 + |\mathcal{P}_f|^2 = 1. \quad (27)$$

With the total polarization vector, the time delay matrix becomes

$$Q = \frac{1}{2} \tau_r (\mathbf{1} + \mathbf{P}_t \cdot \boldsymbol{\sigma}). \quad (28)$$

Since  $(\mathbf{P}_t \cdot \boldsymbol{\sigma})^2 = 1$ , eigenvalues of  $Q$  or total eigentime delays are obtained as zero and  $\tau_r$ , the time delayed by the resonance state. Though time delays due to an avoided crossing interaction and a change in frame transformation are asymmetric with respect to the resonance energy and therefore the energies of the longest lifetimes are not matched with the resonance energy, the energy of the longest overall eigentimes delayed is exactly matched with the resonance energy.

### III. PREPARATION FOR THE GEOMETRICAL REALIZATION

In the previous work, some of the interesting things were noticed but could not be explained. Some of them are summarized below.

- Why are eigenvectors of the  $S$  matrix independent of  $q_a$  while its eigenphase shifts are not?
- Why do the energy behaviors of  $\delta_a(E)$ ,  $\tau_a(E)$ , and  $\tau_f(E)$  follow Beutler-Fano formulas?
- Why does  $\tau_a$  take the Beutler-Fano formula in the energy scale of  $\epsilon_r$  instead of  $\epsilon_a$  in contrast to the case of  $\delta_a$  though the former is obtained as the derivative of the latter.
- Why is  $|\mathbf{P}_a|^2 + |\mathbf{P}_f|^2 = 1$  satisfied?
- What is the meaning of the parameter  $r^2$ ?

In the previous work, we got some help by making an analogy of the system with a spin model, especially in interpreting the time delay matrix  $Q$  with polarization vectors  $\mathbf{P}_a$  and  $\mathbf{P}_f$  which are borrowed from the spin model. But the analogy with the spin model is not fully exploited. Here we show that by exploiting the analogy further, we can give the explanations of the above questions. In particular, we succeeded in giving the geometrical realization of the Beutler-Fano formulas.

Before starting the geometrical realization of the previous results, let us first rewrite some of the previous results suitable for the geometrical realization.

First, we notice that Eqs. (4) and (17) are simpler than the corresponding Eqs. (7) and (18). This indicates that the square root of the Beutler-Fano formula (6) seems to be more fundamental than the original one. Next we notice that Eq. (4) resembles  $\cot \delta_r = -\epsilon_r$  and  $\cot \theta_a = -\epsilon_a$ . Thus the square root of the Beutler-Fano formula may be regarded as an energy parameter  $\epsilon_{\text{BF}}(\epsilon, q, \theta^0)$ . Then Eq. (4) takes the suggestive form

$$\cot \delta_a = -\epsilon_{\text{BF}}(\epsilon_a, q_a, \Delta_{12}^0), \quad (29)$$

where

$$\epsilon_{\text{BF}}(\epsilon_a, q_a, \Delta_{12}^0) = \cot \Delta_{12}^0 \frac{\epsilon_a - q_a}{\sqrt{\epsilon_a^2 + 1}} \quad (30)$$

( $\Delta_{12}^0$  is the value of  $\delta_a$  at  $\epsilon_a \rightarrow -\infty$ ). But there is a one drawback when the square root of the Beutler-Fano formula is considered as an energy parameter. It is not a monotonically increasing function of energy. It has a minimum when  $q > 0$  and a maximum when  $q < 0$ . Hence  $\epsilon_{\text{BF}}$  will be considered here merely as a convenient notation.

Eq. (27) suggests another angle  $\theta_f$  satisfying  $\mathcal{P}_a = \hat{n}_a \cos \theta_f$  and  $\mathcal{P}_f = \hat{n}_f \sin \theta_f$ . Its cotangent is obtained as

$$\cot \theta_f = -\frac{1}{r} \frac{\epsilon_r - q_\tau}{\sqrt{\epsilon_r^2 + 1}}. \quad (31)$$

Eq. (31) indicates that  $1/r$  becomes  $\cot \theta_f$  at  $\epsilon_r \rightarrow -\infty$ . The angle of  $\theta_f$  at  $\epsilon_r \rightarrow -\infty$  is identified with the angle which the polarization vector  $\mathcal{P}_t$  or  $\hat{n}_t$  makes with  $\hat{n}_a$ . That angle will be denoted as  $\theta_t$ . Eq. (26) shows that the angle  $\theta_t$  is obtained as

$$\begin{aligned} \cos \theta_t &= \frac{\Delta\Gamma}{\Gamma}, \\ \sin \theta_t &= \frac{\sqrt{\Gamma^2 - \Delta\Gamma^2}}{\Gamma} \end{aligned} \quad (32)$$

and with it the spherical polar coordinate of  $\hat{n}_t$  is given by  $(1, \theta_t, -\Delta_{12}^0)$ . Now with  $\theta_t$ , Eq. (31) becomes

$$\cot \theta_f = -\cot \theta_t \frac{\epsilon_r - q_\tau}{\sqrt{\epsilon_r^2 + 1}} = -\epsilon_{\text{BF}}(\epsilon_r, q_\tau, \theta_t). \quad (33)$$

With the new angle  $\theta_f$ ,  $\tau_a$  becomes  $\tau_r \cos \theta_f$ , which explains the complicated form of  $\tau_a$  as a functional of the Beutler-Fano function in contrast to that of  $\cot \delta_a$ .

As a result of rewriting, we obtain four equations

$$\begin{aligned} \cot \delta_r &= -\epsilon_r, \\ \cot \theta_a &= -\epsilon_a, \\ \cot \delta_a &= -\epsilon_{\text{BF}}(\epsilon_a, q_a, \Delta_{12}^0), \\ \cot \theta_f &= -\epsilon_{\text{BF}}(\epsilon_r, q_\tau, \theta_t). \end{aligned} \quad (34)$$

The use of the geometrical parameters,  $\delta_r$  and  $\theta_a$ , in place of  $\epsilon_r$  and  $\epsilon_a$  makes the geometrical realization of dynamic relations possible. Our aim is to obtain the dynamic formulas for  $\epsilon_{\text{BF}}(\epsilon_a, q_a, \Delta_{12}^0)$  and  $\epsilon_{\text{BF}}(\epsilon_r, q_\tau, \theta_t)$  by converting the geometric relations containing  $\delta_a$  and  $\theta_f$  back into dynamic ones. We will sometimes abbreviate  $\epsilon_{\text{BF}}(\epsilon_a, q_a, \Delta_{12}^0)$  as  $\epsilon_{\text{BF},a}$  and  $\epsilon_{\text{BF}}(\epsilon_r, q_\tau, \theta_t)$  as  $\epsilon_{\text{BF},r}$ . Before ending this section, let us note the following formulas for the line profile indices  $q_a$  and  $q_\tau$

$$\begin{aligned} q_a &= \frac{\cot \delta_a(\epsilon_a = 0)}{\cot \delta_a(\epsilon_a \rightarrow -\infty)}, \\ q_\tau &= \frac{\cot \theta_f(\epsilon_r = 0)}{\cot \theta_f(\epsilon_r \rightarrow -\infty)}. \end{aligned} \quad (35)$$

They can also be expressed as

$$\begin{aligned} q_a &= \frac{\cot \delta_a}{\cot \Delta_{12}^0} \text{ when } \theta_a = \frac{\pi}{2}, \\ q_\tau &= \frac{\cot \theta_f}{\cot \theta_t} \text{ when } \delta_r = \frac{\pi}{2}. \end{aligned} \quad (36)$$

#### IV. GEOMETRICAL REALIZATION

The geometrical realization is based on that to each unimodular unitary matrix in the complex two-dimensional space, there is an associated real orthogonal matrix representing a rotation in real three-dimensional space [18]. The general two-dimensional unimodular unitary matrix can be written as  $e^{-i\frac{\theta}{2}\boldsymbol{\sigma}\cdot\hat{n}}$  as its determinant can be easily shown to be unity using  $\text{Tr}(\boldsymbol{\sigma}) = 0$  and thus unimodular by the definition of unimodularity. The associated real orthogonal matrix will be denoted as  $R_{\hat{n}}(\theta)$ , the rotation matrix about the vector  $\hat{n}$  by an angle  $\theta$  defined in an active sense.

Let us first consider the  $S$  matrix. It is unitary but not unimodular [ $\det(S) \neq 1$ ] and can not be associated with the pure rotation alone. But after extracting  $\det(S)$  which is equal to  $e^{-i\delta_\Sigma}$  for isolated resonances (a similar formula holds for overlapping resonances, where  $\delta_r$  is replaced by the sum over ones from all resonances [19]), the remaining part of the scattering matrix will be unimodular and may be associated with a pure rotation. According to Eq. (12), the remaining part is  $e^{-i\delta_a \boldsymbol{\sigma} \cdot \hat{n}_a}$  and may be associated with the rotation about the vector  $\hat{n}_a$  by an angle  $2\delta_a$ . We will explore the possibility of this explanation of the  $S$  matrix in below by deriving Eq. (12) in a more systematic way.

In the previous section, the  $S$  matrix was diagonalized by two unitary matrices  $U^0$  and  $V$  given by Eqs. (11) and (9). Actually the theorem in Ref. [20] limits that  $U^0$  and  $V$  are real orthogonal since the  $S$  matrix is symmetric. With them, it is rewritten as

$$S = U^0 V e^{-2i\delta} \tilde{V} \tilde{U}^0. \quad (37)$$

Note that the two unitary transformations  $U^0$  and  $V$  can be written in terms of Pauli spin matrices as

$$\begin{aligned} U^0 &= e^{-i\frac{\theta^0}{2} \boldsymbol{\sigma} \cdot \hat{y}}, \\ V &= e^{-i\frac{\theta_a}{2} \boldsymbol{\sigma} \cdot \hat{y}}. \end{aligned} \quad (38)$$

Notice that argument matrices of two exponential functions are commute and therefore  $U^0 V = e^{-i\frac{1}{2}(\theta_a + \theta^0) \boldsymbol{\sigma} \cdot \hat{y}}$ . As before, let us denote  $\theta_a + \theta^0$  as  $\theta'_a$ . The diagonalized matrix  $e^{-2i\delta}$  of the  $S$  matrix can be expressed in terms of Pauli matrices as

$$e^{-2i\delta} = \begin{pmatrix} e^{-2i\delta_+} & 0 \\ 0 & e^{-2i\delta_-} \end{pmatrix} = e^{-i(\delta_\Sigma \mathbf{1} + \delta_a \boldsymbol{\sigma} \cdot \hat{z})}. \quad (39)$$

Substituting Eqs. (38) and (39) into Eq. (37), we obtain

$$S = e^{-i\frac{\theta'_a}{2} \boldsymbol{\sigma} \cdot \hat{y}} e^{-i(\delta_\Sigma \mathbf{1} + \delta_a \boldsymbol{\sigma} \cdot \hat{z})} e^{i\frac{\theta'_a}{2} \boldsymbol{\sigma} \cdot \hat{y}}. \quad (40)$$

In order to give the geometrical interpretation to Eq. (40), a long preliminary exposition is necessary. Let us start with considering  $\boldsymbol{\sigma} \cdot \mathbf{r}$  and transform it into a new matrix  $\boldsymbol{\sigma} \cdot \mathbf{r}'$  by a general  $2 \times 2$  unitary transformation  $e^{-i\frac{\theta}{2} \boldsymbol{\sigma} \cdot \hat{n}}$  as follows

$$e^{-i\frac{\theta}{2} \boldsymbol{\sigma} \cdot \hat{n}} \boldsymbol{\sigma} \cdot \mathbf{r} e^{i\frac{\theta}{2} \boldsymbol{\sigma} \cdot \hat{n}} = \boldsymbol{\sigma} \cdot \mathbf{r}'. \quad (41)$$

The left hand side of Eq. (41) can be calculated using [21]

$$e^{i\hat{S}} \hat{O} e^{-i\hat{S}} = \hat{O} + i[\hat{S}, \hat{O}] + \frac{i^2}{2!} [\hat{S}, [\hat{S}, \hat{O}]] + \frac{i^3}{3!} [\hat{S}, [\hat{S}, [\hat{S}, \hat{O}]]] + \dots \quad (42)$$

and  $(\boldsymbol{\sigma} \cdot \mathbf{a})(\boldsymbol{\sigma} \cdot \mathbf{b}) = \mathbf{a} \cdot \mathbf{b} + i\boldsymbol{\sigma} \cdot (\mathbf{a} \times \mathbf{b})$  and the result is that  $\mathbf{r}'$  is just the vector obtained from  $\mathbf{r}$  by the three dimensional rotation matrix  $R_{\hat{n}}(\theta)$  about the vector  $\hat{n}$  by  $\theta$  in an active sense as

$$\mathbf{r}' = R_{\hat{n}}(\theta) \mathbf{r}. \quad (43)$$

Only in the form of the similarity transformation (41) the homomorphism that a  $2 \times 2$  unimodular unitary matrix is associated with a three dimensional rotation holds. According to this interpretation, the unitary transformations  $U^0$  and  $V$  for the symmetric  $S$  matrix (37) correspond to the three-dimensional rotations about the  $y$  axis through angles  $\theta^0$  and  $\theta_a$ , respectively, and their overall effect  $U^0 V$  is equal to the rotation about the  $y$  axis by  $\theta'_a = \theta_a + \theta^0$ . Therefore, the original frame transformation for the symmetric  $S$  matrix becomes as a rotation about the  $y$  axis in the ‘‘hypothetical’’ real three-dimensional space. This hypothetical real three-dimensional space is different from the Hilbert space and called the Liouville space. It is the space spanned by the set of vectors  $\sigma_x$ ,  $\sigma_y$ , and  $\sigma_z$  which are orthogonal in the sense that

$$\text{Tr}(\sigma_i \sigma_j) = 2\delta_{ij}, \quad (44)$$

and extensively studied in Ref. [22]. Any traceless  $2 \times 2$  Hermitian matrices, for example  $h$ , can be expanded in this vector space as  $h = x\sigma_x + y\sigma_y + z\sigma_z = (x, y, z) = \boldsymbol{\sigma} \cdot \mathbf{r}$ . We can lift the restriction of traceless in Hermitian matrices if we include the unit matrix  $\mathbf{1}$  as another basic vector in addition to  $\sigma_x$ ,  $\sigma_y$ ,  $\sigma_z$ . Then the three-dimensional Liouville space is a subspace of this four-dimensional Liouville space. Note that two subspace  $\{\mathbf{1}\}$  and  $\{\sigma_x, \sigma_y, \sigma_z\}$  are

orthogonal and therefore either the subspace  $\{\sigma_x, \sigma_y, \sigma_z\}$  or  $\{\mathbf{1}\}$ , or the whole space may be chosen freely depending on the situation without having any trouble.

Now, Eq. (41) can be viewed in two ways. It can be viewed as a rotation of the vector  $\mathbf{r}$  into  $\mathbf{r}'$  by the rotation matrix  $R_{\hat{n}}(\theta)$  as expressed in Eq. (43). Or it can be viewed as the transformation from the  $xyz$  coordinate system to the  $x'y'z'$  coordinate system by the rotation matrix  $R_{\hat{n}}(-\theta)$ . The latter view, though obvious, can be shown to be true using the following mathematical transformation. Let us regard  $\boldsymbol{\sigma}$  and  $\mathbf{r}$  as the column vectors. Then the scalar product  $\boldsymbol{\sigma} \cdot \mathbf{r}'$  can be written as a matrix multiplication of the row vector  $\tilde{\boldsymbol{\sigma}}$  with the column vector  $\mathbf{r}'$ , namely,  $\boldsymbol{\sigma} \cdot \mathbf{r}' = \tilde{\boldsymbol{\sigma}} \mathbf{r}'$ . The support for the view of the coordinate transformation is obtained by the following transformation

$$\tilde{\boldsymbol{\sigma}} \mathbf{r}' = \tilde{\boldsymbol{\sigma}} R_{\hat{n}}(\theta) \mathbf{r} = [\widetilde{R_{\hat{n}}(-\theta)} \boldsymbol{\sigma}] \mathbf{r}. \quad (45)$$

Since the diagonalization of the operator  $\boldsymbol{\sigma} \cdot \mathbf{r}$  yields its eigenchannels, the vector  $\mathbf{r}$  in the three-dimensional Liouville space is enough to uniquely specify the eigenchannels of the traceless Hermitian matrix  $\boldsymbol{\sigma} \cdot \mathbf{r}$ . Conversely, eigenchannels may be regarded as a vector in the three-dimensional Liouville space.

Since any real orthogonal frame transformation is of the form like Eq. (9), it may be generally said that a real orthogonal frame transformation in the complex two-dimensional space corresponds to a rotation about the  $y$  axis in the real three-dimensional Liouville space. Since the matrix corresponding to any  $2 \times 2$  Hermitian operator is diagonal in the basis of eigenchannels by definition of eigenchannels and can be written as  $a\mathbf{1} + b\boldsymbol{\sigma} \cdot \hat{z}$ , a dynamical process along an eigenchannel corresponds to a process along the  $z$  axis in the real three-dimensional Liouville space and leads to a variation in length of the vector. Thus the  $y$  axis in the real three-dimensional Liouville space can be regarded as the axis for the real orthogonal frame transformations and the  $z$  axis as the axis for the dynamical processes along eigenchannels.

We have theorem that  $Ce^B C^{-1} = e^{CBC^{-1}}$  which can be easily proved by using Eq. (42). Using this theorem and Eq. (41), we have

$$e^{-i\frac{\theta}{2}\boldsymbol{\sigma} \cdot \hat{n}} e^{i\boldsymbol{\sigma} \cdot \mathbf{r}} e^{i\frac{\theta}{2}\boldsymbol{\sigma} \cdot \hat{n}} = e^{i\boldsymbol{\sigma} \cdot \mathbf{r}'}. \quad (46)$$

Using Eq. (46) and Eq. (43), Eq. (40) becomes Eq. (12) with  $\hat{n}'_a$  now interpreted as

$$\hat{n}'_a = R_y(\theta'_a) \hat{z}. \quad (47)$$

Or  $\hat{n}'_a$  can be regarded as the  $z'$  axis in the  $x'y'z'$  coordinate system, i.e.,  $\hat{n}'_a = \hat{z}'$ . Let  $S = e^{-2i\boldsymbol{\Delta}'}$ , i.e.,  $\boldsymbol{\Delta}' = \frac{1}{2}(\delta_\Sigma \mathbf{1} + \delta_a \boldsymbol{\sigma} \cdot \hat{n}'_a)$ .  $\boldsymbol{\Delta}'$  is a vector in the four-dimensional Liouville space. Or, if we exclude the isotropic part in  $\boldsymbol{\Delta}'$ ,  $\frac{1}{2}\delta_a \boldsymbol{\sigma} \cdot \hat{n}'_a$  is a vector in the three-dimensional Liouville space which may be obtained by rotating the vector  $\frac{1}{2}\delta_a \boldsymbol{\sigma} \cdot \hat{z}$  about the  $y$  axis by an angle  $\theta'_a$ . The  $\frac{1}{2}\delta_\Sigma \mathbf{1}$  term in  $\boldsymbol{\Delta}'$  gives the phase shift owing to the isotropic influence of the background potential scattering and the resonance on eigenchannels. Likewise, the  $\frac{1}{2}\delta_a \boldsymbol{\sigma} \cdot \hat{n}'_a$  term gives the phase shifts owing to the anisotropic influence of the background scattering potential and the resonance on eigenchannels. Therefore, the length  $\frac{1}{2}\delta_a$  of the anisotropic term in the three-dimensional Liouville space denotes the degree of anisotropic influence on eigenphase shifts by the background scattering and the resonance.

Let us now consider the time delay matrix. If the time delay matrix is written in Lippmann's suggestive form [23],  $Q = S^+ \tau S$  ( $\tau$  is the time operator defined by  $i\hbar \frac{\partial}{\partial E}$ ), it is apparent that the unitary matrix which gives the similarity transformation is now the  $S^+$  matrix and can be associated with the rotation matrix according to the theorem mentioned above when  $\det(S)$  is extracted from it. Using the relation

$$\frac{d^r}{dz^r} (e^{Az}) = A^r e^{Az} = e^{Az} A^r, \quad (48)$$

Eq. (40) is easily differentiated with respect to energy to yield

$$\frac{dS}{dE} = -i \frac{d\delta_\Sigma}{dE} S - i \frac{d\delta_a}{dE} e^{-i\frac{\theta'_a}{2}\boldsymbol{\sigma} \cdot \hat{y}} e^{-i\delta_a \boldsymbol{\sigma} \cdot \hat{z}} \boldsymbol{\sigma} \cdot \hat{z} e^{i\frac{\theta'_a}{2}\boldsymbol{\sigma} \cdot \hat{y}} + \frac{i}{2} \frac{d\theta'_a}{dE} (S \boldsymbol{\sigma} \cdot \hat{y} - \boldsymbol{\sigma} \cdot \hat{y} S). \quad (49)$$

By multiplying (49) with the adjoint of (40), the  $Q$  matrix becomes

$$Q = i\hbar S^+ \frac{dS}{dE} = \hbar \frac{d\delta_\Sigma}{dE} \mathbf{1} + \hbar \frac{d\delta_a}{dE} e^{-i\frac{\theta'_a}{2}\boldsymbol{\sigma} \cdot \hat{y}} \boldsymbol{\sigma} \cdot \hat{z} e^{i\frac{\theta'_a}{2}\boldsymbol{\sigma} \cdot \hat{y}} + \frac{\hbar}{2} \frac{d\theta'_a}{dE} (S^+ \boldsymbol{\sigma} \cdot \hat{y} S - \boldsymbol{\sigma} \cdot \hat{y}), \quad (50)$$

where use is made of the fact that  $S$  is unitary and thus  $S^+ S = 1$  for the first and third terms. The matrix multiplication in the second term of the right hand side of Eq. (50) is just  $\boldsymbol{\sigma} \cdot \hat{n}'_a$  as was already done before. The



sum of the first and second term is the time delay due to the energy derivatives of the eigenphase shifts and called “the partial delay times” by some group of people [5].

The parenthesized part of the third term is the time delay due to the change in frame transformation and has an interference effect between two contributions, one due to the change in frame transformation from the asymptotic channels to the background eigenchannels  $\langle \psi_E^{-(k)} | \psi_E^{(l)} \rangle$  ( $k, l = 1, 2, \dots, n$ ) and the other due to the change in frame transformation from the background eigenchannels to the asymptotic eigenchannels  $\langle \psi_E^{(l)} | \psi_E^{-(m)} \rangle$  ( $l, m = 1, 2, \dots, n$ ). The change in frame transformation does not take place in the direction of the rotation axis given by  $\hat{y}$  but in the rotation angle since the rotation  $y$  axis is fixed in the Liouville space as energy varies. The first contribution has the term  $S^+ \sigma \cdot \hat{y} S$  which is the similarity transformation of the operator  $\sigma \cdot \hat{y}$  by  $S$ . Substituting Eq. (40) for  $S$ , this term becomes

$$S^+ \sigma \cdot \hat{y} S = e^{-i\frac{\theta'_a}{2} \sigma \cdot \hat{y}} e^{i\delta_a \sigma \cdot \hat{z}} \sigma \cdot \hat{y} e^{-i\delta_a \sigma \cdot \hat{z}} e^{i\frac{\theta'_a}{2} \sigma \cdot \hat{y}}, \quad (51)$$

where use is made of that  $e^{i\frac{\theta'_a}{2} \sigma \cdot \hat{y}}$  and  $\sigma \cdot \hat{y}$  are commutative. The scalar factor  $e^{-i\delta_a \sigma \cdot \hat{z}}$  in  $S$  does not appear in Eq. (51) as it is multiplied by its complex conjugation in  $S^+$  to become unity. According to the theorem, the unitary transformations in the right hand side of Eq. (51) correspond to two consecutive rotations, at first about the  $z$  axis by  $-2\delta_a$  and then about the  $y$  axis by  $\theta_a$ . By the first rotation,  $\sigma \cdot \hat{y}$  becomes  $\sigma \cdot (\hat{x} \sin 2\delta_a + \hat{y} \cos 2\delta_a)$ , i.e.,

$$e^{i\delta_a \sigma \cdot \hat{z}} \sigma \cdot \hat{y} e^{-i\delta_a \sigma \cdot \hat{z}} = \sigma \cdot [R_z(-2\delta_a) \hat{y}] = \sigma \cdot (\hat{x} \sin 2\delta_a + \hat{y} \cos 2\delta_a). \quad (52)$$

By substituting Eq. (52) into Eq. (51) and  $\sigma \cdot \hat{y}$ 's being replaced with  $e^{-i\frac{\theta'_a}{2} \sigma \cdot \hat{y}} \sigma \cdot \hat{y} e^{i\frac{\theta'_a}{2} \sigma \cdot \hat{y}}$ ,

$$\begin{aligned} S^+ \sigma \cdot \hat{y} S - \sigma \cdot \hat{y} &= e^{-i\frac{\theta'_a}{2} \sigma \cdot \hat{y}} [\sigma \cdot (\hat{x} \sin 2\delta_a + \hat{y} \cos 2\delta_a) - \sigma \cdot \hat{y}] e^{i\frac{\theta'_a}{2} \sigma \cdot \hat{y}} \\ &= e^{-i\frac{\theta'_a}{2} \sigma \cdot \hat{y}} [2 \sin \delta_a \sigma \cdot (\hat{x} \cos \delta_a - \hat{y} \sin \delta_a)] e^{i\frac{\theta'_a}{2} \sigma \cdot \hat{y}}. \end{aligned} \quad (53)$$

The bracketed part of Eq. (53) is equal to the rotation of the  $x$  axis about the  $z$  axis by  $-\delta_a$  multiplied by  $2 \sin \delta_a$ , which is the overall effect of the interference. Fig. 1 shows this process of interference as a vector addition in the three-dimensional Liouville space. The time delay due to the change in frame transformation, the third term of the right hand side of Eq. (50), becomes

$$\begin{aligned} & \hbar \sin \delta_a \frac{d\theta'_a}{dE} e^{-i\frac{\theta'_a}{2} \sigma \cdot \hat{y}} (\hat{x} \cos \delta_a - \hat{y} \sin \delta_a) e^{i\frac{\theta'_a}{2} \sigma \cdot \hat{y}} \\ &= \hbar \sin \delta_a \frac{d\theta'_a}{dE} e^{-i\frac{\theta'_a}{2} \sigma \cdot \hat{y}} e^{i\frac{\delta_a}{2} \sigma \cdot \hat{z}} \sigma \cdot \hat{x} e^{-i\frac{\delta_a}{2} \sigma \cdot \hat{z}} e^{i\frac{\theta'_a}{2} \sigma \cdot \hat{y}} \\ &= \hbar \sin \delta_a \frac{d\theta'_a}{dE} e^{i\frac{\delta_a}{2} \sigma \cdot \hat{z}'} \sigma \cdot \hat{x}' e^{-i\frac{\delta_a}{2} \sigma \cdot \hat{z}'} \\ &= \hbar \sin \delta_a \frac{d\theta'_a}{dE} \sigma \cdot \hat{x}'', \end{aligned} \quad (54)$$

where the second equality is obtained by applying Eq. (41) twice to the matrix term to obtain  $\sigma \cdot [R_{\hat{y}}(\theta'_a) R_z(-\delta_a) \hat{x}]$  which becomes  $\sigma \cdot R_{\hat{z}'}(-\delta_a) \hat{x}'$  and then by applying Eq. (41) again. In the last equality of Eq. (54), we introduced another new  $x''y''z''$  coordinate system which is obtained from the  $x'y'z'$  coordinate system by the rotation  $R_{\hat{z}'}(\delta_a)$  in the passive sense. In the active sense,  $\hat{x}'' = R_{\hat{z}'}(-\delta_a) \hat{x}'$ .

Substituting Eq. (54) into Eq. (50), the time delay matrix  $Q$  is obtained as

$$Q = \hbar \left( \mathbf{1} \frac{d\delta_\Sigma}{dE} + \sigma \cdot \hat{z}' \frac{d\delta_a}{dE} + \sigma \cdot \hat{x}'' \sin \delta_a \frac{d\theta_a}{dE} \right), \quad (55)$$

and is equal to Eq. (14) when  $\hat{z}'$  and  $\hat{x}''$  are identified with the unit vectors  $\hat{n}'_a$  and  $\hat{n}'_f$  ( $\hat{n}'_{\theta'_a}$  and  $\hat{n}'_{\theta'_a}$  in Ref. [7]) and  $\hbar d\delta_\Sigma/dE$  ( $= \hbar d\delta_r/dE$ ),  $\hbar \sigma \cdot \hat{z}' d\delta_a/dE$ , and  $\hbar \sin \delta_a \sigma \cdot \hat{x}'' d\theta_a/dE$  are identified with  $\frac{1}{2} \tau_r$ ,  $\frac{1}{2} \tau_r \mathbf{P}_a$  and  $\frac{1}{2} \tau_r \mathbf{P}_f$ , respectively. By substituting  $\mathbf{P}_a = \hat{z}' \cos \theta_f = \hat{z}'' \cos \theta_f$  and  $\mathbf{P}_f = \hat{x}'' \sin \theta_f$ , Eq. (55) can also be transformed as follows

$$\begin{aligned} Q &= \frac{1}{2} \tau_r [\mathbf{1} + \sigma \cdot (\hat{z}'' \cos \theta_f + \hat{x}'' \sin \theta_f)] \\ &= \frac{1}{2} \tau_r \left( \mathbf{1} + e^{-i\frac{\theta_f}{2} \sigma \cdot \hat{y}''} \sigma \cdot \hat{z}'' e^{i\frac{\theta_f}{2} \sigma \cdot \hat{y}''} \right) \\ &= \frac{1}{2} \tau_r (\mathbf{1} + \sigma \cdot \hat{z}'''), \end{aligned} \quad (56)$$

where still another  $x'''y'''z'''$  coordinate system is introduced. In the active sense,  $\hat{z}''' = R_{\hat{y}''}(\theta_f)\hat{z}''$ . Eqs. (55) and (56) tells us that time delay matrices due to the avoided crossing interaction, due to the change in frame transformations and the total time delay matrix take simplest form in the  $x'y'z'$ ,  $x''y''z''$ , and  $x'''y'''z'''$  coordinate systems, respectively.

Eq. (56) equals Eq. (28) and therefore  $\hat{z}'''$  equals  $\mathbf{P}_t$ . The vector  $\hat{z}'''$ , and accordingly  $\mathbf{P}_t$ , can be obtained from  $\hat{z}$  by successive rotations by

$$\mathbf{P}_t = \hat{z}''' = R_{\hat{y}''}(\theta_f)R_{\hat{z}'}(-\delta_a)R_{\hat{y}}(\theta'_a)\hat{z} = R_{\hat{y}''}(\theta_f)R_{\hat{y}}(\theta'_a)\hat{z}. \quad (57)$$

As mentioned before, it is better to consider  $\mathbf{P}_t = \tilde{U}^0\mathbf{P}_tU^0$  rather than  $\mathbf{P}_t$  itself since the formula for the former is simpler than that for the latter.  $\mathbf{P}_t$  is the polarization vector pertaining to  $\mathcal{Q} = \tilde{U}^0\mathcal{Q}U^0$  which is the time delay matrix in the basis of background eigenchannel wavefunctions. This suggests that it may be better to take the background eigenchannel wavefunctions rather than the asymptotic channel wavefunctions as a starting channel basis. From now on, let us redefine the  $xyz$  coordinate system as the coordinate system pertaining to the background eigenchannels. Let us use the name of  $x^0y^0z^0$  coordinate system as that pertaining to the asymptotic channels. Definitions of other coordinate systems remain unchanged. With this redefinition of notation, the formulas for  $\mathcal{S}$  and  $\mathcal{Q}$  corresponding to Eqs. (12) and (14) becomes

$$\mathcal{S} = e^{-i\frac{\theta_a}{2}\boldsymbol{\sigma}\cdot\hat{y}}e^{-i(\delta_\Sigma\mathbf{1}+\delta_a\boldsymbol{\sigma}\cdot\hat{z})}e^{i\frac{\theta_a}{2}\boldsymbol{\sigma}\cdot\hat{y}} = e^{-i(\delta_\Sigma\mathbf{1}+\delta_a\boldsymbol{\sigma}\cdot\hat{n}_a)}, \quad (58)$$

$$\mathcal{Q} = \frac{1}{2}(\tau_r\mathbf{1} + \tau_a\boldsymbol{\sigma}\cdot\hat{n}_a + \tau_f\boldsymbol{\sigma}\cdot\hat{n}_f) = \frac{1}{2}\tau_r(\mathbf{1} + \mathbf{P}_a\cdot\boldsymbol{\sigma} + \mathbf{P}_f\cdot\boldsymbol{\sigma}) = \frac{1}{2}\tau_r(\mathbf{1} + \mathbf{P}_t\cdot\boldsymbol{\sigma}), \quad (59)$$

with

$$\begin{aligned} \hat{n}_a &= \hat{z}\cos\theta_a + \hat{x}\sin\theta_a = R_{\hat{y}}(\theta_a)\hat{z}, \\ \hat{n}_f &= \hat{y}\times\hat{n}_a\cos\delta_a - \hat{y}\sin\delta_a = R_{\hat{z}'}(-\delta_a)\hat{x}'. \end{aligned} \quad (60)$$

In place of Eq. (57), we have

$$\mathbf{P}_t = \hat{n}_t = R_{\hat{y}''}(\theta_f)R_{\hat{z}'}(-\delta_a)R_{\hat{y}}(\theta_a)\hat{z} = R_{\hat{y}''}(\theta_f)R_{\hat{y}}(\theta_a)\hat{z}. \quad (61)$$

By substituting the relations  $\cot\theta_a = -\epsilon_a$  and  $\cot\theta_f = -\epsilon_{\text{BF},r}$  into Eq. (61), it is checked that the same formula as Eq. (26) is obtained for  $\hat{n}_t$ . Note that the formula (26) for  $\hat{n}_t$  is independent of energy in contrast to  $\hat{n}_a$  ( $\hat{n}_f$ ) which varies from  $\hat{z}$  ( $\hat{x}$ ) through  $\hat{x}$  ( $-\hat{z}$ ) to  $-\hat{z}$  ( $-\hat{x}$ ) as energy varies from  $-\infty$  to  $\infty$ . This holds generally at least for the multichannel system in the neighborhood of an isolated resonance and derives from the fact that only one type of continua can interact with a discrete state (see Eq. (A6) in Appendix A and Ref. [17] for more general systems).

So far, several coordinate systems are considered such as  $xyz$ ,  $x'y'z'$ ,  $x''y''z''$ , and  $x'''y'''z'''$  coordinate systems pertaining to the eigenchannels of  $S^0$ ,  $S$  or  $\boldsymbol{\sigma}\cdot\mathbf{P}_a$ ,  $\boldsymbol{\sigma}\cdot\mathbf{P}_f$ , and  $\boldsymbol{\sigma}\cdot\mathbf{P}_t$ , respectively. These coordinate systems are shown graphically in Fig. 2. According to Eq. (32), the spherical polar coordinate of  $\hat{n}_t$  is given by  $(1, \theta_t, -\Delta_{12}^0)$  in the  $xyz$  coordinate system. Since  $\hat{n}_a$  lies on the  $xz$  plane, the absolute magnitude  $\Delta_{12}^0$  of the azimuth of  $\hat{n}_t$  is equal to the dihedral angle between two planes whose normals are given by  $\hat{z}\times\hat{n}_a$  and  $\hat{z}\times\hat{n}_t$ . Let us now consider the coordinate of  $\hat{n}_t$  in the  $x'y'z'$  coordinates, where  $\hat{z}' = \hat{n}_a$ . The angle which  $\hat{n}_t$  makes with  $\hat{z}'$  is  $\theta_f$  and the azimuth of  $\hat{n}_t$  may be obtained by considering the  $z'x''$  ( $=z''x''$ ) plane. Note that  $\hat{x}''$  is equal to  $\hat{n}_f$  and  $\hat{n}_t$  lies on the  $z'x''$  plane meaning that the azimuth of  $\hat{n}_t$  is identical with the dihedral angle which the  $z'x''$  plane makes with the  $z'x'$  plane. Since  $x''y''z''$  coordinate system is obtained from  $x'y'z'$  coordinate system by rotating about the  $z'$  axis by  $-\delta_a$ , the dihedral angle which the plane  $z'x''$  makes with the  $z'x'$  plane is  $\delta_a$ . Therefore, the spherical polar coordinate of  $\hat{n}_t$  in the  $x'y'z'$  coordinate system is  $(1, \theta_f, -\delta_a)$ . See Fig. 3 to understand the explanation graphically. Since the dihedral angle between two planes whose normals are  $\hat{n}_a\times\hat{x}'$  and  $\hat{n}_a\times\hat{n}_t$  is  $\delta_a$ , the dihedral angle between two planes whose normals are given by  $\hat{n}_a\times\hat{z}$  and  $\hat{n}_a\times\hat{n}_t$  is  $\pi - \delta_a$ . With this, we can construct a spherical triangle  $\Delta APQ$  with vertices formed with the endpoints of  $\hat{z}$ ,  $\hat{n}_a$ , and  $\hat{n}_t$ , where the vertex angles opposite to the edge angles  $\theta_f$  and  $\theta_t$  are  $\Delta_{12}^0$  and  $\pi - \delta_a$ , respectively, as shown in Fig. 4. The vertex angle opposite to the edge angle  $\theta_a$  can be shown to be  $\delta_r$  by making use of the following relation

$$e^{-i\Delta_{12}^0\boldsymbol{\sigma}\cdot\hat{z}}e^{-i\delta_r\boldsymbol{\sigma}\cdot\hat{n}_t} = e^{-i\delta_a\boldsymbol{\sigma}\cdot\hat{n}_a}, \quad (62)$$

which is the spin model version of the relation  $\mathcal{S} = \mathcal{S}^0(\pi_b + e^{-2i\delta_r}\pi_a)$  (see Appendix A for the derivation). According to Appendix B, Eq. (62) can be expressed using the rotation matrices in the Liouville space as

$$R_{\hat{z}}(2\Delta_{12}^0)R_{\hat{n}_t}(2\delta_r) = R_{\hat{n}_a}(2\delta_a) \quad (63)$$

and manifests that the vertex angle opposite to  $\theta_a$  is  $\delta_r$ .

The dual spherical triangle of  $\Delta$ APQ may be constructed by converting vertices of the original triangle to its edges and edges of the original triangle to its vertices, according to the rule described in Ref. [24]. According to the rule, the vertex angles of the dual spherical triangle are obtained from the corresponding edge angles of the original triangle by subtracting the edge angles from  $\pi$  like  $\pi - \theta_a$ ,  $\pi - \theta_f$  and  $\pi - \theta_t$  and the corresponding edge angles are also obtained similarly like  $\pi - \delta_r$ ,  $\pi - \Delta_{12}^0$  and  $\delta_a$ . The dual spherical triangle constructed in this way is shown in Fig. 5.

Before considering dynamic aspects of the laws holding for the spherical triangle, let us comment on Eq. (62), or the equivalent  $S^0(\pi_b + e^{-2i\delta_r}\pi_a)$ . For this purpose, let us define phase shift matrices  $\Delta^0$ ,  $\Delta_r$ ,  $\Delta$  by  $S^0 = e^{-2i\Delta^0}$ ,  $\pi_b + e^{-2i\delta_r}\pi_a = e^{-2i\Delta_r}$ ,  $S = e^{-2i\Delta}$ . Phase shift matrices are easily obtained as

$$\Delta^0 = \frac{1}{2}(\delta_\Sigma^0 \mathbf{1} + \Delta_{12}^0 \boldsymbol{\sigma} \cdot \hat{z}), \quad (64)$$

$$\Delta_r = \frac{1}{2}(\delta_r \mathbf{1} + \delta_r \boldsymbol{\sigma} \cdot \hat{n}_t), \quad (65)$$

$$\Delta = \frac{1}{2}(\delta_\Sigma \mathbf{1} + \delta_a \boldsymbol{\sigma} \cdot \hat{n}_a). \quad (66)$$

For Eq. (64), if  $\Delta_{12}^0 = 0$ , two eigenchannels have the identical background eigenphase shifts  $\delta_1^0 = \delta_2^0 = \delta_\Sigma^0/2$ . The eigenchannels are isotropic with respect to the potential that brings about the background phase shifts. When two eigenchannels react differently or anisotropically with respect to the potential, eigenchannels have different phase shifts  $\delta_1^0 \neq \delta_2^0$ , or  $\Delta_{12}^0 \neq 0$ . (The off-diagonal term of  $S^0$  gives the transition amplitude and is thus caused by the channel-channel coupling. Since the off-diagonal term is implicitly included in eigenchannels, the potential that eigenchannels feels includes the channel-channel coupling effect.) The anisotropic term of (64) contains the information on this phase difference and the eigenchannels.

The phase shift matrix (64) is a vector whose coordinate is  $(\delta_\Sigma^0, 0, 0, \Delta_{12}^0)$  in the four-dimensional Liouville space. Or, if we consider only the anisotropic term, it is a vector in the three-dimensional Liouville space, whose magnitude is  $\frac{1}{2}\Delta_{12}^0$  and whose direction is  $\hat{z}$ . Though background and resonance scattering contributions appear as a single product term in Eq. (62) in the  $S$  matrix, two contributions are not simply combined in the case of the phase shift matrix  $\Delta$ . For the isotropic parts of two contributions to  $\Delta$ , the combining rule is simple and they are simply added up to give the isotropic part of the phase shift matrix  $\Delta$  as  $\frac{1}{2}\delta_\Sigma = \frac{1}{2}(\delta_\Sigma^0 + \delta_r)$ . The combining rule of anisotropic terms is not so simple. According to the Campbell-Baker-Hausdorff formula [25], the anisotropic part of the phase shift matrix  $\Delta$  is expressed as a very complicated infinite sum of multiple commutators of the anisotropic parts of  $\Delta^0$  and  $\Delta_r$  as

$$\begin{aligned} 2\Delta - \delta_\Sigma \mathbf{1} &= \Delta_{12}^0 \boldsymbol{\sigma} \cdot \hat{z} + \delta_r \boldsymbol{\sigma} \cdot \hat{n}_t - \frac{i}{2} [\Delta_{12}^0 \boldsymbol{\sigma} \cdot \hat{z}, \delta_r \boldsymbol{\sigma} \cdot \hat{n}_t] \\ &\quad - \frac{1}{12} ([[\Delta_{12}^0 \boldsymbol{\sigma} \cdot \hat{z}, \delta_r \boldsymbol{\sigma} \cdot \hat{n}_t], \delta_r \boldsymbol{\sigma} \cdot \hat{n}_t] - [[\Delta_{12}^0 \boldsymbol{\sigma} \cdot \hat{z}, \delta_r \boldsymbol{\sigma} \cdot \hat{n}_t], \Delta_{12}^0 \boldsymbol{\sigma} \cdot \hat{z}]) + \dots \end{aligned} \quad (67)$$

But, the geometrical construction in the Liouville space provides a simple combining rule. For that, at first we ignore the magnitudes of vectors in the three-dimensional Liouville space and consider the spherical triangle made up of endpoints of the unit vectors corresponding to the anisotropic terms. The magnitudes of vectors corresponding to anisotropic terms, instead, are utilized as the edge angles of the spherical triangle. This is the procedure we take when we interpret Eq. (62) as giving the remaining edge angle  $\delta_r$ . Trigonometric laws of the spherical triangle then provide a details of the combining rule which are the subject of the next section.

Let us comment one more thing on the avoided crossing interaction. If we use background eigenchannels as a basis, then the  $S^0$  matrix is already diagonal by definition in that basis. Then for processes occurring along this eigenchannels, there is no channel-channel coupling. If a discrete state is included into the system, background eigenchannels are no longer decoupled and interact each other through the indirect continuum-continuum, or channel-channel, coupling via the discrete state. This indirect channel-channel coupling brings about the avoided crossing interaction in the curves of eigenphase shifts of the  $S$  matrix. Therefore, the avoided crossing interaction is not devoid of the resonance contribution. What is devoid of in the avoided crossing interaction is the isotropic resonant contribution. It includes the anisotropic resonant contribution.

## V. CONNECTION OF THE GEOMETRICAL RELATION WITH DYNAMICS

Now let us describe the dynamical aspects of the geometrical laws holding for the spherical triangle, such as the laws of sines, the laws of cosines. Cotangent laws including four successive parts and laws including five successive parts (see Ref. [26]) are derivable from the laws of sines and cosines but deserve a treatment as separate laws.

Let us consider the cotangent law [26]

$$\sin \Delta_{12}^0 \cot \delta_a = -\sin \theta_a \cot \theta_t + \cos \theta_a \cos \Delta_{12}^0. \quad (68)$$

When  $\cos \theta_a = -\epsilon_a/\sqrt{\epsilon_a^2 + 1}$  and  $\sin \theta_a = 1/\sqrt{\epsilon_a^2 + 1}$  are inserted (for the sign convection, see [27]), Eq. (68) can be put into Beutler-Fano's formula (7) for  $\cot \delta_a$  as follows

$$\begin{aligned} \cot \delta_a &= \frac{1}{\sin \Delta_{12}^0} (\cos \theta_a \cos \Delta_{12}^0 - \sin \theta_a \cot \theta_t) \\ &= -\frac{1}{\sin \Delta_{12}^0} \left( \frac{\epsilon_a}{\sqrt{\epsilon_a^2 + 1}} \cos \Delta_{12}^0 + \frac{1}{\sqrt{\epsilon_a^2 + 1}} \cot \theta_t \right) \\ &= -\cot \Delta_{12}^0 \frac{\epsilon_a - q_a}{\sqrt{\epsilon_a^2 + 1}}, \end{aligned} \quad (69)$$

where  $q_a$  is identified with  $-\cot \theta_t/\cos \Delta_{12}^0$  and can be easily checked to be equal to the previous definition (8) with the use of Eq. (32).

One of the cotangent law for its dual spherical triangle is given by

$$\cot \theta_f \sin \theta_t = -\cos(\pi - \delta_r) \cos \theta_t + \sin(\pi - \delta_r) \cot \Delta_{12}^0. \quad (70)$$

With  $\cos \delta_r = -\epsilon_r/\sqrt{\epsilon_r^2 + 1}$  and  $\sin \delta_r = 1/\sqrt{\epsilon_r^2 + 1}$ , Eq. (70) can be put into Beutler-Fano's formula (33) for  $\cot \theta_f$  as follows

$$\begin{aligned} \cot \theta_f &= \frac{1}{\sin \theta_t} (\cos \delta_r \cos \theta_t + \sin \delta_r \cot \Delta_{12}^0) \\ &= -\frac{1}{\sin \theta_t} \left( \frac{\epsilon_r}{\sqrt{\epsilon_r^2 + 1}} \cos \theta_t - \frac{1}{\sqrt{\epsilon_r^2 + 1}} \cot \Delta_{12}^0 \right) \\ &= -\cot \theta_t \frac{\epsilon_r - q_r}{\sqrt{\epsilon_r^2 + 1}}, \end{aligned} \quad (71)$$

where  $q_r$  is identified with  $\cot \Delta_{12}^0/\cos \theta_t$ , again equal to Eq. (20).

Using Eq. (34) and the convention [27], the sine laws,

$$\begin{aligned} \frac{\sin \Delta_{12}^0}{\sin \theta_f} &= \frac{\sin \delta_r}{\sin \theta_a}, \\ \frac{\sin \delta_r}{\sin \theta_a} &= \frac{\sin \delta_a}{\sin \theta_t} \end{aligned} \quad (72)$$

are translated into

$$\epsilon_a^2 + 1 = \sin^2 \Delta_{12}^0 (\epsilon_r^2 + 1) (\epsilon_{\text{BF},r}^2 + 1), \quad (73)$$

$$\epsilon_r^2 + 1 = \sin^2 \theta_t (\epsilon_a^2 + 1) (\epsilon_{\text{BF},a}^2 + 1), \quad (74)$$

respectively. Eq. (73) was used to derive Eq. (21) in Ref. [7].

(Equating the  $x, y, z$  components of  $\hat{n}_t$  with those of  $\hat{n}_a \cos \theta_f + \hat{n}_f \sin \theta_f$  yields the law involving 5 successive parts  $\sin \theta_t \cos \Delta_{12}^0 = \sin \theta_a \cos \theta_f + \cos \theta_a \sin \theta_f \cos \delta_a$ , one of the laws of sines,  $\sin \Delta_{12}^0/\sin \theta_f = \sin \delta_a/\sin \theta_t$ , and one of the laws of cosines,  $\cos \theta_t = \cos \theta_a \cos \theta_f - \sin \theta_a \sin \theta_f \cos \delta_a$ , in that order. Though such an equality looks irrelevant to the laws of the spherical triangle at a first glance, it actually has to do with the laws of the spherical triangle since it is used to obtain the vertex angle  $\pi - \delta_a$  of the endpoint of  $\hat{n}_a$ .)

The presence of the dual spherical triangle indicates that there is a symmetry with respect to the exchange of vertices and edges. The comparison of the spherical triangle in Fig. 4 with its dual one in Fig. 5 shows that the exchange of  $\delta_r, \theta_f$ , and  $\Delta_{12}^0$  with  $\pi - \theta_a, \delta_a$ , and  $\pi - \theta_t$  transforms the spherical triangle into its dual and vice versa and thus any trigonometric laws will be invariant under this exchange. Besides the geometrical laws, other laws containing not only geometric parameters but also other types of parameters should remain as valid expressions with respect to this exchange. With this requirement, in order for  $\cot \delta_r = -\epsilon_r$  to remain as a valid expression with respect to the exchange,  $\epsilon_r$  should be replaced by  $-\epsilon_a$ . The right hand side of  $q_r = \cot \Delta_{12}^0/\cos \theta_t$  becomes  $\cot \theta_t/\cos \Delta_{12}^0$  which

is equal to  $-q_a$ . Thus  $q_r$  is replaced by  $-q_a$  under the exchange. Similar procedure shows that  $\epsilon_{\text{BF},a}$  is transformed into  $\epsilon_{\text{BF},r}$  under the exchange. The variables with their conjugated ones are summarized in Table I. This symmetry under the exchange yields many relations without derivation thus saves a lot of efforts. It can also be used to check the validity of derived equations. Let us take a few examples. If it holds the relation that

$$\frac{\epsilon_r - q_r}{\sin \theta_t} = \frac{\epsilon_a + \frac{1}{q_a}}{\sin \Delta_{12}^0}, \quad (75)$$

another valid relation is obtained as

$$\frac{\epsilon_a - q_a}{\sin \Delta_{12}^0} = \frac{\epsilon_r + \frac{1}{q_r}}{\sin \theta_t}, \quad (76)$$

by exchanging variables according to Table I. If it holds that

$$\frac{d\delta_a}{d\delta_r} = \cos \theta_f, \quad (77)$$

then the following

$$\frac{d\theta_f}{d\theta_a} = -\cos \delta_a \quad (78)$$

can be obtained by the same procedure.

Geometrical realization reveals that complicated behaviors of dynamical parameters like  $\delta_a$  and  $\theta_f$  as a function of energy are nothing but the result of a simple geometrical traversal along the great circle shown in Fig. 6. Before examining the behaviors of dynamic parameters as functions of energy, it is noted that the vectors  $\hat{z}$  and  $\hat{n}_t$  are fixed in the real three-dimensional Liouville space while  $\hat{n}_a$  changes its direction as energy varies. The constancy of the  $\hat{z}$  vector derives from the usual assumption of energy insensitiveness of background scattering. The constancy of the  $\hat{n}_t$  vector derives from that the time delay matrix has only a resonant contribution as shown in Eq. (A6) and its eigenchannels consist of Fano's energy independent  $\psi_E^{(a)}$  and continua orthogonal to it. As the energy  $\epsilon_r$  varies from  $-\infty$  to  $\infty$ ,  $\theta_a$  undergoes a change from 0 to  $\pi$  which corresponds to the semicircular traversal of the point P from A to the opposite point  $-A$  along the greatest circle while the points A and Q keeps fixed in Fig. 6. In this semicircular traversal, the angle  $\pi - \delta_a$  varies from  $\pi - \Delta_{12}^0$  when P coincides with A to  $\Delta_{12}^0$  when P coincides with  $-A$ . The angle  $\delta_a$ , accordingly, varies from  $\Delta_{12}^0$  to  $\pi - \Delta_{12}^0$ . (The angle  $\theta_f$  varies similarly from  $\theta_t$  to  $\pi - \theta_t$ .) Traversal enjoys a special symmetry when  $\theta_t = \pi/2$ . Let the point A be taken as a polar point. Then the side  $PQ$  becomes part of the equator at the middle of the traversal where  $\theta_a$  becomes  $\pi/2$ . Since any meridian makes the right angle with the equator, the angle  $\delta_a$  which the chord AP makes with the equator becomes a right angle, i.e.,  $\delta_a = \pi/2$ . Now let us consider the deviation of the point P from the equator. Let  $\delta_a = \pi/2 + y$  at  $\theta_a = \pi/2 + x$ . Then, by the symmetry of the spherical triangle,  $\delta_a = \pi/2 - y$  at  $\theta_a = \pi/2 - x$ . Napier's rule

$$\cot \delta_a = \cos \theta_a \cot \Delta_{12}^0 \quad (79)$$

holding for the right spherical triangle satisfies such a symmetry [28]. Obviously,  $q_a = 0$  for Eq. (79). When  $\theta_t \neq \pi/2$ ,  $\delta_a$  is no longer  $\pi/2$  when  $\theta_a = \pi/2$ . The occurrence of the mismatch in energies where values of  $\theta_a$  and  $\delta_a$  become  $\pi/2$  amounts to the addition of  $\sin \theta_a$  term on the right hand side of Eq. (79), which causes the value of  $q_a$  to deviate from zero. The value of  $q_a$  can be obtained as  $-\cot \theta_t / \cos \Delta_{12}^0$  by substituting  $-\cot \theta_t / \sin \Delta_{12}^0$ , one of Napier's rules holding when  $\theta_a = \pi/2$ , for  $\cot \delta_a$  into Eq. (36). It can be roughly stated that the asymmetry of the Beutler-Fano formula for  $\cot \delta_a$  derives from the asymmetry of the geometry.

The concurrent change of  $\theta_f$  with the increase of the arc length  $\theta_a$  as P traverses can be obtained by differentiating the cosine law  $\cos \theta_f = \cos \theta_a \cos \theta_t + \sin \theta_a \sin \theta_t \cos \Delta_{12}^0$  with respect to  $\theta_a$  keeping  $\theta_t$  and  $\Delta_{12}^0$  fixed, which becomes

$$-\sin \theta_f \frac{d\theta_f}{d\theta_a} = -\sin \theta_a \cos \theta_t + \cos \theta_a \sin \theta_t \cos \Delta_{12}^0. \quad (80)$$

The right hand side of Eq. (80) becomes  $-\sin \theta_f \cos(\pi - \delta_a)$  according to the law containing five successive parts, which finally yields

$$\frac{d\theta_f}{d\theta_a} = -\cos \delta_a. \quad (81)$$

Similar derivatives are obtained as

$$\begin{aligned}\frac{d\delta_a}{d\delta_r} &= \cos\theta_f, \\ \frac{d\delta_a}{d\theta_a} &= \cot\theta_f \sin\delta_a, \\ \frac{d\cot\theta_a}{d\cot\delta_r} &= \frac{\sin\Delta_{12}^0}{\sin\theta_t}.\end{aligned}\tag{82}$$

In the spherical triangle  $\Delta ABC$ , Gauss-Bonnet theorem becomes

$$\angle A + \angle B + \angle C = \pi + \frac{\text{area}(\Delta ABC)}{R^2},\tag{83}$$

which states that the sum of interior angles of a spherical triangle exceeds  $\pi$  by the solid angle  $\Omega$  defined by  $\text{area}(\Delta ABC)/R^2$ . In the present case, the sum of interior (vertex) angles is  $\pi + \delta_r + \Delta_{12}^0 - \delta_a$ . Hence, the solid angle  $\Omega$  is

$$\Omega = \delta_r + \Delta_{12}^0 - \delta_a = \delta_r + \delta_\Sigma^0 - 2\delta_2^0 - \delta_a = 2(\delta_- - \delta_2^0).\tag{84}$$

The solid angle of the spherical triangle  $\Delta APQ$  is easily calculated as  $2\Delta_{12}^0$  when the point P coincides with the antipode of A. Then the solid angle of the spherical triangle varies from zero to  $2\Delta_{12}^0$  as the point P varies from the point A to the point  $-A$  and, accordingly,  $\delta_-$  varies from  $\delta_2^0$  to  $\delta_1^0$  as energy varies from  $-\infty$  to  $\infty$ , which is consistent with the result of Ref. [7].

So far, a geometric realization of the  $S$  matrix and  $Q$  matrix has been considered. Let us now go back to the original questions we had in the beginning of Sec. III and see whether we can explain them.

The first of the questions was that the energy variations of the eigenvectors of the  $S$  matrix are independent of  $q_a$  while those of its eigenphase shifts, or more specifically  $\delta_a$ , depend on it. Let us start with that the eigenvectors or eigenchannels of the  $S$  matrix are obtained by the frame transformation of the background eigenchannels. Since the background eigenchannels are fixed, the energy variations of eigenchannels of the  $S$  matrix completely come from the frame transformation which in this case is parametrized with  $\theta_a$ . In Fig. 2,  $\theta_a$  is the edge angle opposite to the vertex angle  $\delta_r$ . If  $\epsilon_r$  varies,  $\delta_r$  varies according to  $\cot\delta_r = -\epsilon_r$ . Since the edge angle  $\theta_a$  is the opposite to  $\delta_r$ ,  $\theta_a$  may be expected to vary linearly with  $\delta_r$ . Such an expectation does not come out right. Instead,  $\cot\theta_a$  varies linearly with  $\cot\delta_r$  according to one of the relations in (82),  $d\cot\theta_a/d\cot\delta_r = \sin\Delta_{12}^0/\sin\theta_t$ , which is fixed in energy. The relation tells us that  $\cot\theta_a$  has a linear relation with  $\epsilon_r$  but  $\cot\theta_a$  may not be zero when  $\epsilon_r = 0$ , in general. But, we can always introduce a new energy scale, let us call it  $\epsilon_a$ , where  $\cot\theta_a$  is zero at  $\epsilon_a = 0$  and the proportionality constant can be set so that  $\cot\theta_a = -\epsilon_a$ . The argument proves that  $\cot\theta_a$  does not need no further parameter like  $q_a$ . The reason why the energy variation of  $\delta_a$  needs the line profile index is already considered around Eq. (79) and need not be repeated here.

If the second question which asks why the energy behaviors of  $\delta_a$ ,  $\tau_a$  and  $\tau_f$  follow the Beutler-Fano formulas is changed like ‘‘is it possible to show geometrically that their behaviors follow the Beutler-Fano formula?’’, the answer is yes and their behavior is the result of the cotangent laws holding for the spherical triangle, as we have done in this section.

Let us answer the third question why  $\tau_a$  takes the Beutler-Fano formula in the energy scale of  $\epsilon_r$  instead of  $\epsilon_a$  though  $\tau_a$  is obtained as the derivative of  $\epsilon_a$ . Note that the question on  $\tau_a$  can be paraphrased to that on  $\cot\theta_f$  since  $\tau_a = \tau_r(\epsilon_r)(1 + \cot^2\theta_f)^{-1/2}$ . There are two such cotangent laws for  $\cot\theta_f$  as follows

$$\cot\theta_f = \frac{1}{\sin\theta_t} (\cos\delta_r \cos\theta_t + \sin\delta_r \cot\Delta_{12}^0),\tag{85}$$

$$\cot\theta_f = \frac{1}{\sin\theta_a} (-\cos\delta_a \cos\theta_a + \sin\delta_a \cot\Delta_{12}^0).\tag{86}$$

Eq. (85) expresses  $\cot\theta_f$  in terms of  $\epsilon_r$  while Eq. (86) expresses it in terms of  $\epsilon_a$ . In Eq. (85),  $\delta_r$  is the only parameters which is a function of energy while, in Eq. (86), not only  $\delta_a$  but also  $\theta_a$  are parameters which are functions of energy. Eq. (85) gives the Beutler-Fano formula as a function of  $\epsilon_r$  as we already saw in Eq. (71). Eq. (86) might also give a Beutler-Fano formula as a function of  $\epsilon_a$  if  $\theta_a$  were a constant of energy but it fails to do so as  $\theta_a$  is a function of energy, too. On the other hand, if  $\theta_t$  were a function of energy, Eq. (85) could not give the Beutler-Fano formula, too. This argument reveals that cotangent laws of a spherical triangle alone are not sufficient to guarantee the presence of Beutler-Fano formulas.

Let us consider the answer to the fourth question which asks the reason why  $|\mathbf{P}_t|^2 = |\mathbf{P}_a|^2 + |\mathbf{P}_f|^2 = 1$  is satisfied. Eq. (A6) shows that non-zero resonant behavior of time delay occurs only when the system is in the  $\psi_E^{(a)}$  state, which derives from that the  $\psi_E^{(a)}$  state is the only type of continuum which can interact with the discrete state. On the other hand, the unit magnitude of the polarization  $\mathbf{P}_t$  means that only one continuum shows a resonant behavior while others do not. Thus Eq. (A6) proves that  $|\mathbf{P}_t| = 1$ .

The answer to the fifth question is provided by the identification of  $r^2$  with  $\tan^2 \theta_t^2$  and need not be considered further.

## VI. APPLICATION TO THE TRIATOMIC VAN DER WAALS PREDISSOCIATION

Ref. [7] and the present paper have developed the theory for the behaviors of eigenphase shifts and time delays. Let us now consider the application of the theory to the vibrational predissociation of triatomic van der Waals molecules. The theory can be applied in two ways. When the  $S$  matrix is known as a function of energy either experimentally or by a theoretical calculation, eigenphase shifts can be calculated directly by its diagonalization. Similarly, eigentime delays can be calculated from the  $S$  matrix. For these data, formulas for eigenphase shifts and time delays derived from the theory can be used as models with parameters in the formulas viewed as adjustable ones. Extracting best values of the parameters may be tried by fitting the data of eigenphase shifts and eigentime delays obtained by the diagonalization of the  $S$  matrix to the theoretical models. On the other hand, by using the formulas for the parameters themselves derived from the theory, parameters can be directly calculated without doing data fitting. Parameters obtained in two different ways, namely, by data-fitting and by using the theoretical formulas are not identical as the theory developed so far relies on the assumption that background eigenphase shifts and partial decay widths are constants of energy, which is usually a good approximation but does not hold exactly in the actual system.

The data-fitting will be done only for the eigentime delay sum (22) and partial delay times  $2\hbar d\delta_+/dE$  and  $2\hbar d\delta_-/dE$ . Eigenphase shifts will not be used for the data-fitting since they need the information on  $E_a$  and  $\Gamma_a$ , which is not available before the data-fitting. The data-fitting of partial delay times to the theoretical formulas

$$\begin{aligned} 2\hbar \frac{d\delta_{\pm}}{dE} &= \hbar \left( \frac{d\delta_r}{dE} \pm \frac{d\delta_a}{dE} \right) = \frac{1}{2}(\tau_r \pm \tau_a) = \frac{1}{2}\tau_r(1 \pm \cos \theta_f) \\ &= \frac{2\hbar}{\Gamma} \frac{1}{1 + \epsilon_r^2} \left[ 1 \mp \frac{\epsilon_r - q_r}{\sqrt{(\epsilon_r - q_r)^2 + \tan^2 \theta_t (1 + \epsilon_r^2)}} \right] \end{aligned} \quad (87)$$

can be easily done on the other hand since the information on  $E_0$  and  $\Gamma$  which are necessary to convert  $E$  to  $\epsilon_r$  needed for Eq. (87) can be easily obtained from the data-fitting of the eigentime delay sum (22). (Eigenphase sum can also be used to get  $E_0$  and  $\Gamma$ .)

Graphs of partial delay times are shown in Fig. 7 for several values of line profile indices. Some general characteristics of the graphs are noticed.

1. Graphs of partial delay times  $2\hbar d\delta_+/dE$  and  $2\hbar d\delta_-/dE$  meet at  $\epsilon_r = q_r$ .
2. As  $|q_r| \rightarrow \cot \Delta_{12}^{\circ}$ ,

$$\cos \theta_f(\epsilon_r) \rightarrow \begin{cases} 1 & \text{when } \epsilon_r \leq q_r \\ -1 & \text{when } \epsilon_r > q_r, \end{cases} \quad (88)$$

and the partial delay times becomes

$$\begin{aligned} 2\hbar \frac{d\delta_+}{dE} &\rightarrow \begin{cases} \tau_r(\epsilon_r) & \text{when } \epsilon_r \leq q_r \\ 0 & \text{when } \epsilon_r > q_r, \end{cases} \\ 2\hbar \frac{d\delta_-}{dE} &\rightarrow \begin{cases} 0 & \text{when } \epsilon_r \leq q_r \\ \tau_r(\epsilon_r) & \text{when } \epsilon_r > q_r. \end{cases} \end{aligned} \quad (89)$$

This case corresponds to  $\theta_t \rightarrow 0$ , or  $\theta_f \rightarrow \theta_a$ , as can be easily seen from the inspection of Fig. 6. But with this geometrical consideration alone, it is hard to find the limit of  $\cos \theta_f$  in Eq. (88). The behavior of the limit of  $\cos \theta_f$  can only be obtained when  $\Gamma_a \rightarrow 0$  is taken into account at  $\theta_t \rightarrow 0$ , i.e., when the strength of the channel

coupling is taken into account, which is hidden in the geometrical consideration because of the use of  $\epsilon_a$ . When  $\Gamma_a \rightarrow 0$ ,

$$\epsilon_a \rightarrow \begin{cases} -\infty & \text{when } E < E_a \\ \infty & \text{when } E > E_a. \end{cases} \quad (90)$$

Only two values of  $\epsilon_a$  are possible in the limit of  $\Gamma_a \rightarrow 0$  or  $|q_\tau| \rightarrow \cot \Delta_{12}^0$ .  $\epsilon_a \rightarrow \mp \infty$  correspond to  $\theta_a \rightarrow 0$  and  $\pi$ , or  $\cos \theta_a \rightarrow 1$  and  $-1$ , respectively. Since  $\cos \theta_f \rightarrow \cos \theta_a$ ,  $\cos \theta_f$  satisfies the limit (88) as  $|q_\tau| \rightarrow \cot \Delta_{12}^0$ . The energies at which  $\cos \theta_f$  and  $\epsilon_a$  undergo abrupt changes look different but are equivalent since  $E = E_a$  or  $\epsilon_a = 0$  corresponds to  $\epsilon_r = q_\tau$  owing to the relation (75) and  $q_a \rightarrow \infty$ .

3. As  $|q_\tau| \rightarrow \infty$ , the graph of  $\cos \theta_f(\epsilon_r)$  becomes symmetric with respect to origin and is given by

$$\cos \theta_f(\epsilon_r) \rightarrow \frac{\cos \Delta_{12}^0}{\sqrt{\epsilon_r^2 \sin^2 \Delta_{12}^0 + 1}} \text{ when } |q_\tau| \rightarrow \infty. \quad (91)$$

The derivation of Eq. (91) from Eq. (87) is not so easy.  $|q_\tau| \rightarrow \infty$  arises in two cases,  $\cot \Delta_{12}^0 \rightarrow \infty$  or  $\cos \theta_t = 0$  ( $\theta_t = \pi/2$ ). The geometric consideration is a great help when  $\theta_t = \pi/2$ . In this case, Napier's rule gives  $\cot \theta_f = \sin \delta_r \cot \Delta_{12}^0$  [28]. From this formula of  $\cot \theta_f$ ,  $\cos^2 \theta_f = \cos^2 \Delta_{12}^0 / (\epsilon_r^2 \sin^2 \Delta_{12}^0 + 1)$  is obtained by simple trigonometric manipulations. The square roots of both sides of it yields Eq. (91) except for the sign. In order to fix the sign, let us consider the case of  $\epsilon_r = 0$  which corresponds to  $\delta_r = \pi/2$ . Since  $\theta_t = \delta_r = \pi/2$  means that the chord PQ in Fig. 6 is part of the equator, we have  $\theta_a = \delta_a = \pi/2$ . For this particular spherical triangle, it can be easily proved that  $\theta_f = \Delta_{12}^0$ . This fixes the sign. The remaining case of  $\cot \Delta_{12}^0 \rightarrow \infty$  corresponds to  $\Gamma_a \rightarrow 0$  and can not be easily handled by geometric argument as mentioned above. Eq. (74) of Ref. [7] allows us to handle this case and yields  $\cos \theta_f = \cos \Delta_{12}^0$  which is identical with Eq. (91) in this case.

The partial delay times at  $\epsilon_r = 0$  are

$$\begin{aligned} 2\hbar \frac{d\delta_+}{dE}(\epsilon_r = 0) &\rightarrow \frac{4\hbar}{\Gamma} \cos^2 \left( \frac{\Delta_{12}^0}{2} \right), \\ 2\hbar \frac{d\delta_-}{dE}(\epsilon_r = 0) &\rightarrow \frac{4\hbar}{\Gamma} \sin^2 \left( \frac{\Delta_{12}^0}{2} \right), \end{aligned} \quad (92)$$

which is easily obtained by substituting  $\Delta_{12}^0$  for  $\theta_f$  into  $2\hbar d\delta_\pm/dE = \tau_r(1 \pm \cos \theta_f)$ .

Before doing the data-fitting, let us briefly describe the system used for the calculation and the methods of calculation. A triatomic van der Waals molecule considered here is of the type of rare gas  $\cdots$  homonuclear halogen-like diatomic molecules [31]. Let us consider the system where the van der Waals molecule in its ground state is excited by the light whose energy amounts to the excitation of the diatomic vibronic motion from the  $v = 0$  to 1 state. This energy is sufficient to break the van der Waals bond and produces a predissociation spectrum as the energy of light is scanned over a certain range of frequency.

The following interaction potential between A and B<sub>2</sub> in A  $\cdots$  B<sub>2</sub> triatomic system

$$V(R, r, \gamma) = \begin{cases} V_M(R, r, \gamma) & \text{when } R \leq R^* \\ V_{\text{vdW}}(r, \gamma) + (V_M - V_{\text{vdW}})e^{-\rho \left( \frac{R-R^*}{R^*} \right)^2} & \text{when } R \geq R^*, \end{cases} \quad (93)$$

is the one employed by Halberstadt et. al. to fit the predissociation data for Ne  $\cdots$  Cl<sub>2</sub> system and is used here [32]. In Eq. (93),  $R, r, \gamma$  are the Jacobi coordinates that denote the distance between A and the center of mass of B<sub>2</sub>, the bond distance of B<sub>2</sub>, and the angle between  $\mathbf{R}$  and  $\mathbf{r}$ , respectively [33];  $V_M(R, r, \gamma)$  and  $V_{\text{vdW}}$  are given as

$$V_M(R, r, \gamma) = D_{\text{AB}} \sum_{i=1}^2 \left\{ \left[ e^{-\alpha_{\text{AB}}(R_{\text{AB}_i} - R_{\text{AB}}^{(o)})} - 1 \right]^2 - 1 \right\}^2 \quad (94)$$

$$+ D_{\text{CM}} \left\{ \left[ e^{-\alpha_{\text{CM}}(R - R_{\text{CM}}^{(o)})} - 1 \right]^2 - 1 \right\}^2, \quad (95)$$

$$V_{\text{vdW}}(R, \gamma) = -\frac{C_6(\gamma)}{R^6} - \frac{C_8(\gamma)}{R^8}, \quad (96)$$



where  $R_{AB_i}$  is the distance between A and  $i^{\text{th}}$  B atom; other parameters are adjusted parameters to yield the best fit to the experimental values. The values of the parameters used in this paper are given in Table II. Two Legendre terms are retained for  $C_6(\gamma)$  and  $C_8(\gamma)$  in Eq. (96), e.g.,

$$C_6(\gamma) = C_{60} + C_{62}P_2(\cos \gamma). \quad (97)$$

$R^*$  in Eq. (93) is chosen as the inflection point of the atom-atom Morse potentials and given by  $R^* = R_{\text{CM}}^{(o)} + \ln 2 / \alpha_{\text{CM}}$ .

The Hamiltonian for the triatomic van der Waals molecules  $A \cdots B_2$  in the Jacobi coordinates is given in atomic units by [32]

$$H = -\frac{1}{2m} \frac{\partial^2}{\partial R^2} + \frac{\mathbf{j}^2}{2\mu r^2} + \frac{\mathbf{l}^2}{2mR^2} + V(R, r, \gamma) + H_{B_2}(r), \quad (98)$$

where

$$H_{B_2}(r) = -\frac{1}{2\mu r^2} \frac{\partial^2}{\partial r^2} + V_{B_2}(r), \quad (99)$$

denotes the vibrational Hamiltonian of  $B_2$ ;  $m$  is the reduced mass of  $B_2$ ;  $\mu$  denotes the reduced mass of A and the center of mass of  $B_2$ ;  $\mathbf{j}$  is the angular momentum operator of  $B_2$ ;  $\mathbf{l}$  is the orbital angular momentum operator of the relative motion of A and the center of mass of  $B_2$ . The values of diatomic molecular parameters of  $B_2$  used in this paper are given in Table III. The calculation is limited to zero of the total angular momentum operator  $\mathbf{J} = \mathbf{j} + \mathbf{l}$ , as usually done in this field without affecting the predissociation dynamics much. Such a limitation simplifies the Hamiltonian as  $\mathbf{l}$  can be replaced by  $\mathbf{j}$ .

Let  $\Psi^{-(i)}(R, r, \gamma)$  be the eigenfunctions of  $H$  of Eq. (98) and let it correspond to the state vibronically excited by light which will be predissociating into an atom and a diatomic fragment. It is indexed by the vib-rotational quantum numbers  $(v, j)$  of its diatomic photo-fragment and abbreviated to  $i$ , i.e.,  $i = (v, j)$ . When the wavefunctions  $\Psi^{-(i)}(R, r, \gamma)$  to the dissociation channel  $i = (v, j)$  are expanded in terms of  $n$  base functions  $\Phi_{i'}(r, \gamma) = (r|v')Y_{j'o}(\gamma, 0)$  ( $i' = 1, 2, \dots, n$ ) as

$$\Psi^{-(i)}(R, r, \gamma) = \sum_{i'} \Phi_{i'}(r, \gamma) \chi_{i'i}(R), \quad (100)$$

the close-coupling equations for  $\chi_{i'i}(R)$  are obtained as

$$\left[ -\frac{1}{2m} \frac{d^2}{dR^2} - k_{i'}^2 + \frac{\mathbf{j}^2}{2mR^2} \right] \chi_{i'i}(R) + \sum_{i''} V_{i'i''}(R) \chi_{i''i}(R) = 0, \quad (101)$$

with

$$k_{i'}^2 = 2m[E - B j'(j' + 1) - (v' + \frac{1}{2})\omega], \quad (102)$$

and

$$V_{i''i'}(R) = \int d\gamma \sin \gamma \int dr \Phi_{i''}(r, \gamma) V(R, r, \gamma) \Phi_{i'}^*(r, \gamma). \quad (103)$$

The close-coupling equation (101) is solved by the De Vogelaere algorithm [34] and wavefunctions (100) that satisfy the incoming wave boundary condition are, consequently, obtained. The  $S$  matrix obtained in this process, which is identical with (2), is diagonalized and eigenphase shifts (3) are obtained. Two closed channels corresponding to  $(v = 1, j = 0)$  and  $(v = 1, j = 2)$  and two open channels corresponding to  $(v = 0, j = 0)$  and  $(v = 0, j = 2)$  are included to mimic the system of one discrete state and two continua to which the theory developed in this work applies. This calculation yields the data of eigenphase shifts as functions of energy. Let us call this method of calculation as the close-coupling method.

Note that the theory developed in Ref. [7] and in the present paper relies on the presence of a discrete state embedded in continua. Among various theories devised to describe the resonance with explicit consideration of a discrete state, Fano's configuration interaction theory is chosen in this work [7]. In the normal use as described in the above paragraph, the close-coupling method can not be connected with the configuration interaction theory since no discrete state is assumed in the close-coupling method. But with a little modification in its use, it can be used

to calculate dynamic parameters of the configuration interaction theory. A discrete state with its resonance energy  $E_0$  used in the configuration interaction theory can be obtained by solving the close-coupling equations (modified to incorporate the shooting method [35]) with inclusion of closed channels alone. Wavefunctions obtained by solving the close-coupling equations with inclusion of open channels alone obviously diagonalize the Hamiltonian in the subspace spanned by open channels alone and are the continuum wavefunctions  $\psi_E^{-(l)}$  considered in the configuration interaction theory. The background scattering matrix  $S^0$  are obtained as a byproduct when the continuum wavefunctions  $\psi_E^{-(l)}$  are forced to satisfy the incoming wave boundary conditions (or outgoing wave boundary condition if a scattering system is considered instead of the photo-dissociation). By diagonalizing  $S^0$ , background eigenphase shifts  $\delta_1^0$  and  $\delta_2^0$  and the frame transformation matrix  $U^0$  from the asymptotic wavefunctions  $\psi_E^{-(l)}$  to background eigen channel wavefunctions  $\psi_E^{(k)}$  are obtained. With  $U^0$ , background eigenchannel wavefunctions can be obtained from the asymptotic ones as

$$\psi_E^{(k)}(R, r, \gamma) = -ie^{i\delta_k^0} \sum_l \tilde{U}_{kl}^0 \psi_E^{-(l)}(R, r, \gamma), \quad (104)$$

and can be used to calculate partial decay width  $\Gamma_k$  as

$$\Gamma_k = 2\pi \left| \left( \psi_E^{(k)} | H | \phi \right) \right|^2 = 2\pi \left| \left( \psi_E^{(k)} | V(R, r, \gamma) | \phi \right) \right|^2, \quad (105)$$

where the last equality holds for  $\delta v = \pm 1$  vibronic predissociation since  $V(R, r, \gamma)$  is the only term containing odd powers of  $r$  in  $H$ . Since  $E_0$ ,  $\delta_1^0$ ,  $\delta_2^0$ ,  $\Gamma_1$ , and  $\Gamma_2$  are obtained, the dynamic parameters  $E_a$ ,  $\Gamma_a$ ,  $q_a$ ,  $q_\tau$ , and  $\cot \theta_t$  are calculated using  $E_a = E_0 + \Delta\Gamma \cot \Delta_{12}^0/2$ ,  $\Gamma_a = 2\sqrt{\Gamma_1\Gamma_2}/\sin \Delta_{12}^0$ , Eqs. (8), (20), and (32).

Though the configuration interaction theory directly calculates the dynamic parameters  $E_0$ ,  $\Gamma$ ,  $E_a$ ,  $\Gamma_a$ ,  $q_a$ ,  $q_\tau$ , and  $\cot \theta_t$ , the close-coupling method can not calculate them directly. Dynamical parameters directly obtainable from the close-coupling method are the  $S$  matrix, its eigenphase shifts  $\delta_+$  and  $\delta_-$ , and partial delay times  $2\hbar d\delta_+/dE$  and  $2\hbar d\delta_-/dE$  as functions of energy. If the assumptions used in configuration interaction theory are exact, eigenphase shifts and partial delay times should satisfy Eq. (3) and Eq. (87), respectively. The assumptions that  $\delta_1^0$ ,  $\delta_2^0$ ,  $\Gamma_1$ , and  $\Gamma_2$  are constant of energy on which the configuration interaction theory relies are expected not to cause much trouble in the actual situation as far as the energy range is not wide enough. If eigenphase shifts and partial delay times follow Eq. (3) and Eq. (87), values of dynamic parameters  $E_a$ ,  $\Gamma_a$ ,  $q_a$ ,  $q_\tau$ , and  $\cot \theta_t$  can be obtained by varying them so that eigenphase shifts and partial delay times calculated by the close-coupling method fit the formulas best. Fitting is done with the Levenberg-Marquardt method recommended for the nonlinear models in Ref. [35]. For the reason mentioned above, only partial delay times will be fitted.

Data fittings are done in two steps. At first,  $E_0$  and  $\Gamma$  are obtained by fitting the eigentime delay sum. Then  $q_\tau$  and  $\cot \theta_t$  are obtained by fitting partial delay times  $2\hbar d\delta_+/dE$  ( $=\tau_r + \tau_a$ ) and  $2\hbar d\delta_-/dE$  ( $=\tau_r - \tau_a$ ) with (87). Either  $2\hbar d\delta_+/dE$  or  $2\hbar d\delta_-/dE$  can be used to obtain the values of  $q_\tau$  and  $\cot \theta_t$ . Values of  $q_\tau$  and  $\cot \theta_t$  obtained from either of them should be identical if the assumption of the configuration interaction method, namely that  $\Gamma_1$ ,  $\Gamma_2$ ,  $\delta_1^0$ , and  $\delta_2^0$  are constant of energy, is exact. The differences between  $q_\tau$ 's and  $\cot \theta_t$ 's for  $2\hbar d\delta_+/dE$  and  $2\hbar d\delta_-/dE$  may serve as a criterion of the exactness of the configuration interaction theory.

Numerical study shows that fitting the eigentime delay sum calculated by the close-coupling method to the formula (22) is done reliably. Compared with that, fitting the partial delay times to the formula (87) can not be easily done. Eigentime delays calculated by the close-coupling method show abnormal behaviors like negative values of eigentime delays at the energy region not far from a resonance while theory contends that eigentime delays are positive in the neighborhood of a resonance, meaning that assumptions made for the formula (87) are prone to break down. It may be argued that parameters obtained by data-fitting of eigentime delays calculated by the close-coupling method will deviate more from those obtained by the configuration interaction method as the range of energy taken for fitting is wider. But we can not always narrow the range of energy for this reason. Notice that  $q_\tau$  is the energy where  $\tau_+$  meets  $\tau_-$ . As seen in Eq. (89), if  $q_\tau$  is large, two curves are almost identical with  $\tau_r$  except for the neighborhood of  $q_\tau$ . Therefore for the good fitting, the energy range taken for fitting should include  $q_\tau$ . It means that if  $q_\tau$  is large, fitting is likely to be bad. This assertion is checked by doing data-fittings for three different ranges of energy, namely,  $[E_0 - \Gamma, E_0 + \Gamma]$ ,  $[E_0 - 2\Gamma, E_0 + 2\Gamma]$ , and  $[E_0 - 3\Gamma, E_0 + 3\Gamma]$ .

Table IV shows the results calculated with the parameters given in Table II and III. Table V is obtained with the same parameters but with  $r_e = 5.044$  a.u. The former table corresponds to the case of large  $q_\tau$  while the latter table to the case of small  $q_\tau$ . The tables also show values of a fudge factor  $\lambda$  which can be used as a criteria for the goodness-of-fit. The fitting is done at first by steepest decent method with the initial value, say 0.001, of  $\lambda$ . New value of  $\lambda$  is suggested for the next iteration. If the suggested value of  $\lambda$  becomes sufficiently small, inverse-Hessian method is used for fitting. At the final call,  $\lambda$  is set to zero. This method assumes that values of  $\lambda$  should approach zero if everything goes O.K. This is true with the data-fitting of the eigentime delay sum. For the partial delay times,

values of  $\lambda$  do not go to zero. Though values of  $\lambda$  do not go to zero, comparison of curves obtained by two method showed that the fitting is good enough to be acceptable if values of  $\lambda$  are not too large. In Table IV, the values of  $q_\tau$  lies beyond the first interval  $[E_o - \Gamma, E_o + \Gamma]$  and lies in the second interval. According to the reasons mentioned above, it is hard to achieve reliable data-fitting in this case. The closest result to the theoretical values is obtained for the first interval, the narrowest one, where the fudge factor is worst indicating wider interval should be used. The calculation shows that wider interval yields worse result indicating that the assumptions may no longer be true. On the other hand, in Table V, the value of  $q_\tau$  is small and the data-fitting may be done rather reliably and is confirmed by the calculation. This situation contrasts greatly to the fitting of partial photo-dissociation cross-sections to the Fano-Beutler-like line profile formulas [29]

$$\sigma_j = \sigma_j^\circ \frac{|\epsilon + q_j|^2}{1 + \epsilon^2} = \sigma_j^\circ \frac{[\epsilon + \Re(q_j)]^2}{1 + \epsilon^2} + \sigma_j^\circ \frac{[\Im(q_j)]^2}{1 + \epsilon^2}, \quad (106)$$

for the same predissociating system of van der Waals molecules, where the fitting is excellent as shown in Table VI.

## VII. SUMMARY AND DISCUSSION

In the previous work [7], eigenphase shifts for the  $S$  matrix and Smith's lifetime matrix  $Q$  near a resonance were expressed as functionals of the Beutler-Fano formulas using appropriate dimensionless energy units and line profile indices. Parameters responsible for the avoided crossing of eigenphase shifts and eigentime delays and the change in frame transformation in the eigentime delays were identified. The geometrical realization of those dynamical parameters is tried in this work, which allows us to give a geometrical derivation of the Beutler-Fano formulas appearing in eigenphase shifts and time delays.

The geometrical realization is based on the real three-dimensional space spanned by the Pauli matrices  $\sigma_x, \sigma_y, \sigma_z$  as basic vectors, where vectors are orthogonal in the sense that

$$\text{Tr}(\sigma_i \sigma_j) = 2\delta_{ij}. \quad (107)$$

Such a kind of space is called a Liouville space [22]. A  $2 \times 2$  traceless Hermitian matrix, which is generally expressed as  $\boldsymbol{\sigma} \cdot \mathbf{r}$  with  $\mathbf{r}$  real, is a vector in this Liouville space. The magnitude of a vector in the three-dimensional Liouville space corresponds to the degree of anisotropy in coupling of eigenchannels with the cause that brings about the dynamics of the dynamic operator corresponding to the vector. The four-dimensional Liouville space including the unit matrix  $\mathbf{1}$  as another basic vector is also used for the  $2 \times 2$  Hermitian matrix whose trace is not zero.

Resonant scattering can be separated from the background scattering in the  $\mathcal{S}$  matrix for the multichannel system around an isolated resonance as  $\mathcal{S} = \mathcal{S}^0(\pi_b + e^{-2i\delta_r}\pi_a)$  where  $\pi_a$  is the projection matrix to  $\psi_E^{(a)}$  which is the only type of continua interacting with the discrete state and  $\pi_b = 1 - \pi_a$  [30]. When the number of open channels are limited to two,  $\mathcal{S}^0$ ,  $\pi_b + e^{-2i\delta_r}\pi_a$ , and  $\mathcal{S}$  can be expressed using Pauli's spin matrices as

$$\begin{aligned} \mathcal{S}^0 &= e^{-i(\delta_\Sigma^0 \mathbf{1} + \Delta_{12}^0 \boldsymbol{\sigma} \cdot \hat{z})}, \\ \pi_b + e^{-2i\delta_r}\pi_a &= e^{-i(\delta_r \mathbf{1} + \delta_r \boldsymbol{\sigma} \cdot \hat{n}_t)}, \\ \mathcal{S} &= e^{-i(\delta_\Sigma \mathbf{1} + \delta_a \boldsymbol{\sigma} \cdot \hat{n}_a)}. \end{aligned}$$

Phase shift matrices  $\Delta^0$ ,  $\Delta_r$ , and  $\Delta$  which are Hermitian may be defined for  $\mathcal{S}^0$ ,  $\pi_b + e^{-2i\delta_r}\pi_a$ , and  $\mathcal{S}$  as

$$\begin{aligned} \Delta^0 &= \frac{1}{2}(\delta_\Sigma^0 \mathbf{1} + \Delta_{12}^0 \boldsymbol{\sigma} \cdot \hat{z}), \\ \Delta_r &= \frac{1}{2}(\delta_r \mathbf{1} + \delta_r \boldsymbol{\sigma} \cdot \hat{n}_t), \\ \Delta &= \frac{1}{2}(\delta_\Sigma \mathbf{1} + \delta_a \boldsymbol{\sigma} \cdot \hat{n}_a) \end{aligned}$$

and are vectors in the four-dimensional Liouville space.

According to the Campbell-Baker-Hausdorff formula, the phase shift matrix  $\Delta$  is expressed as an infinite sum of multiple commutators of  $\Delta^0$  and  $\Delta_r$ , which is difficult to use [25]. The geometric way of representing the combining rule of  $\Delta^0$  and  $\Delta_r$  into  $\Delta$  provides an alternative to that. We first note that the isotropic part  $\frac{1}{2}\delta_\Sigma$  of  $\Delta$  is simply obtained from those of  $\Delta^0$  and  $\Delta_r$  as a simple addition  $\frac{1}{2}(\delta_\Sigma^0 + \delta_r)$  and factored out in  $\mathcal{S} = \mathcal{S}^0(\pi_b + e^{-2i\delta_r}\pi_a)$ . Then the remaining anisotropic part of  $\Delta$  is obtained from those of  $\Delta^0$  and  $\Delta_r$  as

$$e^{-i\Delta_{12}^0 \boldsymbol{\sigma} \cdot \hat{\mathbf{z}}} e^{-i\delta_r \boldsymbol{\sigma} \cdot \hat{\mathbf{n}}_t} = e^{-i\delta_a \boldsymbol{\sigma} \cdot \hat{\mathbf{n}}_a}.$$

The above identity can be expressed using the rotation matrices in the Liouville space as

$$R_{\hat{\mathbf{z}}}(2\Delta_{12}^0)R_{\hat{\mathbf{n}}_t}(2\delta_r) = R_{\hat{\mathbf{n}}_a}(2\delta_a).$$

This relation leads to the construction of the spherical triangle whose vertices are the endpoints of vectors corresponding to the anisotropic parts of the phase shift matrices but whose lengths are limited to unity. The lengths of the vectors are utilized as the vertex angles of the spherical triangle. This spherical triangle shows the rule of combining the channel-channel couplings in the background scattering with the resonant interaction to give the avoided crossing interactions in the curves of eigenphase shifts as functions of energy.

The time delay matrix  $\mathcal{Q}$  basically derives from the energy derivative of the phase shift matrix  $\mathbf{\Delta}$  of the  $\mathcal{S}$  matrix. The phase shift matrix  $\mathbf{\Delta}$  is a vector in the four-dimensional Liouville space and is  $\frac{1}{2}(\delta_\Sigma \mathbf{1} + \delta_a \boldsymbol{\sigma} \cdot \hat{\mathbf{n}}_a)$  as stated above. The energy derivative of  $\delta_\Sigma$  and  $\delta_a$  without changing the direction of the vector  $\hat{\mathbf{n}}_a$  yields the ‘‘partial delay time matrix’’ given by  $\hbar(d\delta_{1\Sigma}/dE + \boldsymbol{\sigma} \cdot \hat{\mathbf{n}}_a)d\delta_a/dE$ . Discussion on the time delay matrix due to a change in the direction of the vector  $\hat{\mathbf{n}}_a$  or in frame transformation is greatly facilitated by the use of the formula  $\frac{1}{2}\hbar(d\theta_a/dE)(\mathcal{S}^+ \boldsymbol{\sigma} \cdot \hat{\mathbf{y}}\mathcal{S} - \boldsymbol{\sigma} \cdot \hat{\mathbf{y}})$ . The formula shows that the time delay due to the change in frame transformation is the interference of two terms. The first term inside the parenthesis comes from the energy derivative of the frame transformation from the background eigenchannels to the  $\mathcal{S}$  matrix eigenchannels and the second term from the energy derivative of the frame transformation from the  $\mathcal{S}$  matrix eigenchannels to the background eigenchannels. The first term corresponds to a vector rotated from the  $\hat{\mathbf{y}}$  vector by the rotation  $R_{\hat{\mathbf{n}}_a}(-2\delta_a)$ . The net time delay resulted from the interference is thus calculated by the vector addition in the three-dimensional Liouville space.

Going back to the spherical triangle, the laws of sines and cosines and other laws derivable from such laws such as the laws of cotangents holding for the spherical triangle can be translated into dynamic laws by converting  $\delta_r$  and  $\theta_a$  into energies according to  $\cot \delta_r = -\epsilon_r$  and  $\cot \theta_a = -\epsilon_a$ . Two cotangent laws

$$\begin{aligned} \sin \Delta_{12}^0 \cot \delta_a &= -\sin \theta_a \cot \theta_t + \cos \theta_a \cos \Delta_{12}^0, \\ \cot \theta_f \sin \theta_t &= -\cos(\pi - \delta_r) \cos \theta_t + \sin(\pi - \delta_r) \cot \Delta_{12}^0, \end{aligned}$$

can be shown to correspond to two Beutler-Fano formulas for  $\cot \delta_a$  and  $\cot \theta_f$

$$\begin{aligned} \cot \delta_a &= -\cot \Delta_{12}^0 \frac{\epsilon_a - q_a}{\sqrt{\epsilon_a^2 + 1}}, \\ \cot \theta_f &= -\cot \theta_t \frac{\epsilon_r - q_r}{\sqrt{\epsilon_r^2 + 1}}, \end{aligned}$$

with such conversion. Other laws also yields interesting relations among dynamical parameters.

The presence of the dual triangle of the spherical triangle indicates that we can make a one-to-one correspondence between edge angles with vertex angles so that if there is one valid relation we can make another valid relation by interchanging angles with its one-to-one corresponding angles. In other words, for each edge angle, we have a conjugate vertex angle and vice versa. This conjugation relation can be extended to  $\epsilon_r$  and  $\epsilon_a$  by making use of their relation with  $\delta_r$  and  $\theta_a$ , respectively. The full conjugation relations among geometrical and dynamical parameters are listed Table I. The duality of the spherical triangle thus explains the symmetry found in the dynamic relations and provides us with a systematic approach and complete symmetric relations. Besides this use of trigonometric laws of the spherical triangle, the geometric construction in the Liouville space facilitates other useful consideration.

Note that the geometrical laws holding for the geometrical objects in the real three-dimensional Liouville space deal only with the intrinsic nature of the dynamic couplings independent of the characteristics of the individual system. It derives from that the reduced energies hide the specific characteristics of the dynamic couplings of the individual system such as the strengths of the dynamic couplings between the discrete state and continua, the indirect couplings between continua via discrete states, the resonance positions, the avoided crossing point energy. Intrinsic nature of the dynamic couplings is concerned with the relations among eigenchannels for various dynamic operators, the anisotropy in the channels coupling in the  $S^0$  and  $S$  scattering, the anisotropy in the channel coupling with the discrete state. This shows both the beauty and the limitations of the geometrical construction in the Liouville space. In the actual application, we have to be careful when considering the case close to the limits in coupling strength, where abnormal behaviors take place in actual dynamic quantities, but where no abnormality shows up in the Liouville space.

The present theory is developed for the system of one discrete state and two continua. It will be desirable to extend the theory to more than two open channels and to overlapping resonances for which the results of Refs. [17,19] will be a great help. It might be also valuable to apply the present theory to MQDT. In connection with the latter, it might be interesting to apply the present theory to extend the Lu-Fano plot to multi-open channel case.

## ACKNOWLEDGMENTS

This work was supported by KOSEF under contract No. 961-0305-050-2 and by Korean Ministry of Education through Research Fund No. 1998-015-D00186.

- [1] P. G. Burke, J. Cooper, and S. Ormonde, *Phys. Rev.* **183**, 245 (1969); C. J. Goebel and K. W. McVoy, *Phys. Rev.* **164**, 1932 (1967).
- [2] D.W. Schwenke and D.G. Truhlar, *J. Chem. Phys.* **87**, 1095 (1987); S.W. Cho, A.F. Wagner, B. Gazdy, and J.M. Bowman, *ibid.* **96**, 2812 (1992).
- [3] U. Fano and A. R. P. Rau, *Atomic Collisions and Spectra* (Academic, Orlando, 1986).
- [4] See, for example, Eqs. (45) and (57) in U. Fano, *Phys. Rev. A* **2**, 353 (1970)
- [5] Y. Fyodorov and H. -J. Sommers, *J. Math. Phys.* **38**, 1918 (1997) and references therein.
- [6] J. Macek, *Phys. Rev. A* **2**, 1101 (1970).
- [7] C. W. Lee, *Phys. Rev. A* **58**, 4581 (1998).
- [8] See, for example, J. R. Taylor, *Scattering Theory* (John Wiley and Sons, New York, 1972); Appendix B of C. W. Lee, *Bull. Korean Chem. Soc.* **16**, 850 (1995).
- [9] The terminology ‘‘asymptotic channel wavefunctions’’ is used for  $\psi_E^{-l}$  ( $l = 1, 2, \dots, n$ ) which satisfy the incoming wave boundary conditions. The ‘‘background eigenchannel wavefunctions’’ are the eigenvectors  $\psi_E^{(k)}$  of the  $S^0$  matrix and related to  $\psi_E^{-l}$  by  $\psi_E^{(k)} = -ie^{i\delta_k^0} \sum_l \tilde{U}_{kl}^0 \psi_E^{-l}$  where  $U^0$  is defined as  $S^0 = U^0 e^{-2i\delta^0} \tilde{U}^0$ .
- [10] U. Fano, *Phys. Rev.* **124**, 1866 (1961).
- [11] A. U. Hazi, *Phys. Rev. A* **19**, 920 (1979).
- [12] F. T. Smith, *Phys. Rev.* **118**, 349 (1960).
- [13]  $Q$  matrix in terms of  $S$  matrix can take various forms depending on which boundary conditions, incoming or outgoing, are used and how  $S$  matrix is defined. The relation  $Q = i\hbar S^+ dS/dE$  used in this paper corresponds to the incoming wave boundary condition with the  $S$  matrix defined by  ${}_{\infty}\psi_j = \Phi_j - \sum_k \Phi_k^* S_{kj}$  where  $\Phi_j$  is the outgoing wave  $v_j^{-1/2} e^{ik_j x} \omega_j(y)$ . Smith used the outgoing wave boundary condition with  $S_{jk}$ 's multiplying  $\Phi_k$  in front of it and obtained the different relation  $Q = i\hbar S dS^+/dE$ . For notations and derivation, see Ref. [12].
- [14] Without losing generality, the convention that  $0 \leq \Delta_{12}^0 \leq \pi$  and  $0 \leq \theta_t \leq \pi$  is chosen so that  $\sin \Delta_{12}^0 \geq 0$  and  $\sin \theta_t \geq 0$ . The convention  $\sin \theta_t \geq 0$  ensures that  $\sin \theta_f \geq 0$  and  $\tau_f = \tau_r \sin \theta_f \geq 0$  since  $\theta_t \leq \theta_f \leq \pi - \theta_t$ .
- [15] L. Eisenbud, Ph. D thesis, Princeton, June, 1948 (unpublished).
- [16] M. L. Goldberger and K. M. Watson, *Collision Theory* (John Wiley and Sons, New York, 1964); T. Omura, *Progr. Theor. Phys. Suppl.* **29**, 108 (1964); R. Fong, *Phys. Rev. B* **140**, 762 (1965); M. Bauer, P. A. Mello, and K. W. McVoy, *Z. Physik A* **293**, 151 (1979); R. Landauer and Th. Martin, *Rev. Mod. Phys.* **66**, 217 (1994); C. Bracher and M. Kleber, *Ann. Physik* **4**, 696 (1995).
- [17] V. L. Lyuboshitz, *Phys. Lett* **72B**, 41 (1977).
- [18] See, for example, M. Tinkham, *Group Theory and Quantum Mechanics* (McGraw-Hill, New York, 1964), p104.
- [19] M. Simonius, *Phys. Lett.* **52B**, 279 (1974).
- [20] U. Fano and G. Racah, *Irreducible Tensorial Sets* (Academic, New York, 1959), the footnote of p 134.
- [21] See, for example, E. Merzbacher, *Quantum Mechanics* (John Wiley and Sons, New York, 1998), p 39.
- [22] U. Fano, *Rev. Mod. Phys.* **29**, 74 (1957); also see U. Fano and A. R. P. Rau, *Symmetries in Quantum Physics* (Academic, San Diego, 1996).
- [23] B. A. Lippmann, *Phys. Rev.* **151**, 1023 (1966).
- [24] G. A. Jennings, *Modern Geometry with Applications* (Springer, New York, 1994), Chap. 2.
- [25] G. H. Weiss and A. A. Maradudin, *J. Math. and Phys.* **3**, 771 (1962); R. M. Wilcox, *J. Math. Phys.* **8**, 962 (1967); A. N. Richmond, in *Applications of Matrix Theory*, edited by M. J. C. Gover and S. Barnett (Oxford, Oxford, 1989).
- [26] See, for example, C. H. Chiang, *Kinematics of Spherical Mechanisms* (Cambridge, Cambridge, 1988), p351.
- [27] The convention of  $\cos \theta = -\epsilon/\sqrt{\epsilon^2 + 1}$  and  $\sin \theta = 1/\sqrt{\epsilon^2 + 1}$  mentioned in Ref. [7] is employed for relations  $\cot \theta = -\epsilon$  like  $\cot \delta_r = -\epsilon_r$ ,  $\cot \theta_a = -\epsilon_a$ ,  $\cot \delta_a = -\epsilon_{BF,a}$ ,  $\cot \delta_r = -\epsilon_{BF,r}$ .
- [28] The dual spherical triangle in Fig. 5 becomes a right triangle when  $\theta_t = \pi/2$ , for which Napier's rule holds [26]. According to Napier's rule, the sine of any middle part of the circular form given by

$$\left( (\theta_f - \frac{\pi}{2})(\pi - \delta_r)(\pi - \Delta_{12}^0)(\theta_a - \frac{\pi}{2})(\frac{\pi}{2} - \delta_a) \right)$$

is the product of the tangents of the adjacent parts. Eq. (79) is obtained by choosing  $\theta_a - \pi/2$  as the middle part.

- [29] C.W. Lee, Bull. Korean Chem. Soc. **16**, 850 (1995).  
 [30] U. Fano and J.W. Cooper, Phys. Rev. A **137**, 1364 (1965).  
 [31] See, for example, G. Delgado-Barrio and J. A. Beswick, in *Structure and Dynamics of Non-Rigid Molecular Systems*, edited by Y. G. Smeyers (Kluwer Academic Publishers, Dordrecht, 1995) and references therein.  
 [32] N. Halberstadt, J. A. Beswick, and K. C. Janda, J. Chem. Phys. **87**, 3966 (1987).  
 [33] J. A. Beswick and J. Jortner, Adv. Chem. Phys. **47**, 363 (1981).  
 [34] W. Lester, Methods. Comput. Phys. **10**, 243 (1971).  
 [35] W. H. Press, S. A. Teukolsky, W. T. Vetterling and B. P. Flannery, *Numerical Recipes in C* (Cambridge, New York, 1992).

## APPENDIX A: SEPARATION OF THE RESONANT CONTRIBUTION FROM THE BACKGROUND ONE IN $S$ MATRIX

The  $S$  matrix for the multichannel system in the neighborhood of an isolated resonance given in Eq. (2) can also be written as

$$S_{jk} = \sum_l S_{jl}^0 \left( \delta_{lj} + 2\pi i \frac{V_{lE} V_{kE}^*}{E - E_0 - i\Gamma/2} \right), \quad (\text{A1})$$

where  $V_{lE}$  is defined in terms of the asymptotic state  $\psi_E^{-(j)}$  as  $(\psi_E^{-(j)} | H | \phi)$ . Using the relation  $(E - E_0 + i\Gamma/2)/(E - E_0 - i\Gamma/2) = e^{-2i\delta_r}$ , Eq. (A1) becomes

$$S_{jk} = \sum_l S_{jl}^0 \left[ \delta_{lj} + (e^{-2i\delta_r} - 1) \frac{2\pi}{\Gamma} V_{lE} V_{kE}^* \right]. \quad (\text{A2})$$

If we consider Fano's  $\psi_E^{(a)}$  state defined as

$$|\psi_E^{(a)}\rangle = \sqrt{\frac{2\pi}{\Gamma}} \sum_j |\psi_E^{-(j)}\rangle V_{jE}, \quad (\text{A3})$$

and the projection operator  $|\psi_E^{(a)}\rangle\langle\psi_E^{(a)}|$  into that state, and define the projection matrix  $\Pi_a$  whose  $(l, j)$  element is given by

$$(\Pi_a)_{lj} = \langle\psi_E^{-(l)}|\psi_E^{(a)}\rangle\langle\psi_E^{(a)}|\psi_E^{-(j)}\rangle = \frac{2\pi}{\Gamma} V_{lE} V_{jE}^*, \quad (\text{A4})$$

Eq. (A2) becomes in matrix form as

$$S = S^0 + (e^{-2i\delta_r} - 1) S^0 \Pi_a = S^0 (\Pi_b + e^{-2i\delta_r} \Pi_a), \quad (\text{A5})$$

where  $\Pi_b$  is equal to  $1 - \Pi_a$  and is the projection matrix into the space orthogonal to the space of  $\psi_E^{(a)}$  and may be regarded as a projection matrix into the background. Using Eq. (A5), the time delay matrix  $Q$  becomes

$$Q = 2\hbar \frac{d\delta_r}{dE} \Pi_a. \quad (\text{A6})$$

Notice that Fano's  $\psi_E^{(a)}$  and other continua orthogonal to it are the eigenstates of the time delay matrix  $Q$  for the multichannel system in the neighborhood of an isolated resonance.

Now let us confine the number of open channels of the system to 2. Then the background scattering matrix  $S^0$  and projection matrices  $\Pi_a$  and  $\Pi_b$  in Eq. (A5) and (A6) can be expressible in terms of Pauli matrices. When we convert them into ones in terms of Pauli matrices, it may be convenient to choose the background eigenstates as a basis. Let us denote the background scattering matrix and projection operators in the basis of background eigenstates as  $\mathcal{S}^0$ ,  $\pi_a$ , and  $\pi_b$ . They can be obtained from those in the basis of asymptotic channel wavefunctions as  $\tilde{U}^0 S^0 U^0$ ,  $\tilde{U}^0 \Pi_a U^0$ ,  $\tilde{U}^0 \Pi_b U^0$ , respectively. Eqs. (A5) and (A6) are now in the basis of background eigenchannels as follows

$$S = \mathcal{S}^0 (\pi_b + e^{-2i\delta_r} \pi_a), \quad (\text{A7})$$

$$Q = 2\hbar \frac{d\delta_r}{dE} \pi_a. \quad (\text{A8})$$

Now in the basis of the background eigenchannels the background scattering matrix  $\mathcal{S}^0$  takes the form

$$\mathcal{S}^0 = \begin{pmatrix} e^{-2i\delta_1^0} & 0 \\ 0 & e^{-2i\delta_2^0} \end{pmatrix} = e^{-i(\delta_\Sigma^0 \mathbf{1} + \Delta_{12}^0 \boldsymbol{\sigma} \cdot \hat{z})}. \quad (\text{A9})$$

Comparing Eq. (59) and Eq. (A8), we obtain

$$\pi_a = \frac{1}{2} (\mathbf{1} + \boldsymbol{\sigma} \cdot \hat{n}_t), \quad (\text{A10})$$

from which  $\pi_b$  is obtained as

$$\pi_b = \frac{1}{2} (\mathbf{1} - \boldsymbol{\sigma} \cdot \hat{n}_t). \quad (\text{A11})$$

Inserting Eqs. (A10) and (A11) into Eq. (A7), we obtain

$$\mathcal{S} = e^{-i(\delta_\Sigma^0 \mathbf{1} + \Delta_{12}^0 \boldsymbol{\sigma} \cdot \hat{z})} e^{-i(\delta_r \mathbf{1} + \delta_r \boldsymbol{\sigma} \cdot \hat{n}_t)}. \quad (\text{A12})$$

Equating Eqs. (58) and (A12), Eq. (62) is obtained.

## APPENDIX B: MULTIPLICATION OF TWO ROTATIONS AND SPHERICAL TRIANGLE

Multiplication of two rotations yields another rotation. The question is how the three rotations are related geometrically in real three-dimensional space. If three rotations are represented by three rotation axes  $\hat{n}_A$ ,  $\hat{n}_B$ ,  $\hat{n}_C$  and corresponding three rotation angles  $2A$ ,  $2B$ ,  $2\pi - 2C$ , we found that three rotation axis form a spherical triangle whose vertex angles are given by  $A$ ,  $B$ , and  $C$  (the corresponding opposite edge angles will be denoted as  $a$ ,  $b$ , and  $c$ ). When this theorem is expressed in terms of unitary matrices in the complex two dimensional space, it takes the form

$$e^{-iA\boldsymbol{\sigma} \cdot \hat{n}_A} e^{-iB\boldsymbol{\sigma} \cdot \hat{n}_B} = e^{-i(\pi-C)\boldsymbol{\sigma} \cdot \hat{n}_C}. \quad (\text{B1})$$

The proof of this theorem can easily be done if we use the relation  $e^{-ia\boldsymbol{\sigma} \cdot \hat{n}} = \cos a - i\boldsymbol{\sigma} \cdot \hat{n} \sin a$  and various sine and cosine laws of the spherical triangle and will be omitted. The similarity transformation  $e^{-i(\pi-C)\boldsymbol{\sigma} \cdot \hat{n}_C} h e^{i(\pi-C)\boldsymbol{\sigma} \cdot \hat{n}_C}$  is equal to  $e^{-iB\boldsymbol{\sigma} \cdot \hat{n}_B} e^{-iA\boldsymbol{\sigma} \cdot \hat{n}_A} h e^{iA\boldsymbol{\sigma} \cdot \hat{n}_A} e^{iB\boldsymbol{\sigma} \cdot \hat{n}_B}$  owing to the identity (B1). Such an equality of two similarity transformation can be expressed in terms of rotation matrices as

$$R_{\hat{n}_A}(2A)R_{\hat{n}_B}(2B) = R_{\hat{n}_C}(-2C). \quad (\text{B2})$$

Sometimes, it might be convenient if rotations in the identity (B1) are expressed in terms of basic axes instead of arbitrary ones. Without losing generality, let us take  $\hat{n}_A$  as the  $z$  axis and let  $\hat{n}_B$  lie on the  $zx$  plane. Then the spherical polar coordinates of three vectors are  $\hat{n}_A = (1,0,0)$ ,  $\hat{n}_B = (1,c,0)$ , and  $\hat{n}_C = (1,b,A)$ . Using  $R_{\hat{n}_B}(2B) = R_{\hat{y}}(c)R_{\hat{z}}(2B)R_{\hat{y}}(-c)$  and similar formula for  $R_{\hat{n}_C}(-2C)$ , Eq. (B2) becomes

$$R_{\hat{n}_A}(2A)R_{\hat{y}}(c)R_{\hat{z}}(2B)R_{\hat{y}}(-c) = R_{\hat{z}}(A)R_{\hat{y}}(b)R_{\hat{z}}(-2C)R_{\hat{y}}(-b)R_{\hat{z}}(-A). \quad (\text{B3})$$

The validity of Eq. (B3) can be proved by inserting the explicit formula for the rotation matrices, for example, such as

$$R_{\hat{z}}(\theta) = \begin{pmatrix} \cos \theta & -\sin \theta & 0 \\ \sin \theta & \cos \theta & 0 \\ 0 & 0 & 1 \end{pmatrix}, \quad (\text{B4})$$

and by using sine and cosine laws of spherical triangle, the derivation of which is straightforward but requires patience. The equality of two relations (B2) and (B3) can be shown using the finite rotation formula for the vector  $\mathbf{r}'$  which is obtained by rotating  $\mathbf{r}$  about the unit vector  $\hat{n}$  through an angle  $\Phi$  as follows

$$\mathbf{r}' = \hat{n}(\hat{n} \cdot \mathbf{r}) + [\mathbf{r} - \hat{n}(\hat{n} \cdot \mathbf{r})] \cos \Phi + (\mathbf{r} \times \hat{n}) \sin \Phi. \quad (\text{B5})$$

TABLE I. Conjugate variables.

Variable	Conjugate variable
$\delta_r$	$\pi - \theta_a$
$\theta_f$	$\delta_a$
$\Delta_{12}^0$	$\pi - \theta_t$
$\epsilon_r$	$-\epsilon_a$
$\epsilon_{BF,r}$	$\epsilon_{BF,a}$
$q_\tau$	$-q_a$

TABLE II. Parameters for the model intermolecular system  $A \cdots B_2$ .

Parameter	Value
Reduced mass between A and B <sub>2</sub>	
m	6756.8 a.u.
Morse potential parameters	
$D_{AB}$	0.0034 eV
$\alpha_{AB}$	1.0 a.u. <sup>-1</sup>
$R_{AB}^{(o)}$	6.82 a.u.
$D_{CM}$	0.00195 eV
$\alpha_{CM}$	1.0 a.u. <sup>-1</sup>
$R_{CM}^{(o)}$	6.65 a.u.
Van der Waals potential parameters	
$C_{60}$	0.75 eV(a.u.) <sup>-6</sup>
$C_{62}$	0.119 eV(a.u.) <sup>-6</sup>
$C_{80}$	1.58 eV(a.u.) <sup>-8</sup>
$C_{82}$	0.8 eV(a.u.) <sup>-8</sup>

TABLE III. Diatomic molecular parameters.

Parameter	Value
vibrational frequency	$\omega_e$ 0.0162 eV
rotational constant	$B$ 0.01758 meV
equilibrium bond length	$r_e$ 3.044 a.u.
reduced mass	$\mu$ 32576.6 a.u.



TABLE IV. Comparison of parameters obtained from the theory in this paper and from the data-fitting of partial delay times calculated by the close-coupling method. The channels included in the close-coupling equation are described in the text. Values of parameters in Tables II and III are used in the calculation. The three energy intervals used for the data-fitting in the close-coupling method correspond to  $[-2, 2]$ ,  $[-4, 4]$ , and  $[-6, 6]$ , respectively, in  $\epsilon_r$  scale. In this system,  $\cot^2 \theta_t \gg 1$  and  $\theta_t \approx -\pi$ . This means that  $q_\tau \approx -\cot \Delta_{12}^0$ , corresponding to the limiting case considered in Eq. (89). Note that  $q_\tau$  lies in the second interval  $[-4, -2]$  beyond the first interval. The avoided crossing point energy  $E_a$  is located at  $-4.4 \times 10^{-6}$  eV from the resonance energy  $E_0$  and is very close to  $q_\tau$  when measured in  $\epsilon_r$  scale since it is equal to  $q_\tau \cos^2 \theta_t$ .  $\sin \theta_t \approx 0$  means that  $\Gamma_2 \approx 0$ , physically corresponding to the system where the decay process into one open channel is much faster than that into another open channel.

	Theory in this paper	Close-coupling method		
		$[E_0 - \Gamma, E_0 + \Gamma]$	$[E_0 - 2\Gamma, E_0 + 2\Gamma]$	$[E_0 - 3\Gamma, E_0 + 3\Gamma]$
$E_0$ (eV)	0.01396397	0.01396567	0.01396567	0.01396567
$\Gamma$ (eV)	$2.38 \times 10^{-6}$	$2.35 \times 10^{-6}$	$2.34 \times 10^{-6}$	$2.320 \times 10^{-6}$
		$2\hbar \frac{d\delta_+}{dE}$		
$q_\tau$	-3.69	-3.56	-3.25	-3.45
$\cot^2 \theta_t$	5274	5000	$1.0 \times 10^5$	$2.7 \times 10^5$
$\lambda$		$10^{-1}$	$10^{-9}$	$10^{-4}$
		$2\hbar \frac{d\delta_-}{dE}$		
$q_\tau$	-3.69	-3.56	-3.40	-3.51
$\cot^2 \theta_t$	5274	5000	$5.9 \times 10^4$	$-1.4 \times 10^4$
$\lambda$		$10^{-1}$	$10^{-3}$	$10^{-5}$

TABLE V. Comparison of parameters obtained from the theory in this paper and from the data-fitting of the partial delay times calculated by the close coupling method. The channels included in the close-coupling equation and values of parameters used in the calculation are the same as those in Table IV except that  $r_e = 5.044$  a.u. Avoided crossing point energy is located at  $8.1 \times 10^{-8}$  eV from the resonance energy and lies very close to the resonance energy, meaning that  $\Delta_{12}^0 \approx \pi/2$ . Then  $q_\tau \sim 0$ .

	Theory in this paper	Close-coupling method		
		$[E_0 - \Gamma, E_0 + \Gamma]$	$[E_0 - 2\Gamma, E_0 + 2\Gamma]$	$[E_0 - 3\Gamma, E_0 + 3\Gamma]$
$E_0$ (eV)	0.01553487	0.01553486	0.01553486	0.01553486
$\Gamma$ (eV)	$3.35 \times 10^{-6}$	$3.29 \times 10^{-6}$	$3.27 \times 10^{-6}$	$3.24 \times 10^{-6}$
		$2\hbar \frac{d\delta_+}{dE}$		
$q_\tau$	0.115	0.164	0.199	0.254
$\cot^2 \theta_t$	0.73	0.71	0.75	0.78
$\lambda$		$10^{-8}$	$10^{-5}$	$10^{-5}$
		$2\hbar \frac{d\delta_-}{dE}$		
$q_\tau$	0.115	0.109	0.132	0.133
$\cot^2 \theta_t$	0.73	0.71	0.74	0.77
$\lambda$		$10^{-3}$	$10^{-7}$	$10^{-3}$

TABLE VI. Comparison between line profile indices of partial photo-dissociation cross sections obtained by the configuration theory and by the close-coupling method. Adopted from Ref. [29].

$j$	Configuration interaction method			Close-coupling method		
	$\sigma_j^o$ [arb. unit]	$\Re(q_j)$	$[\Im(q_j)]^2$	$\sigma_j^o$ [arb. unit]	$\Re(q_j)$	$[\Im(q_j)]^2$
0	0.221	-356	24280	0.219	-358	24920
2	0.279	-233	169	0.281	-233	-48
4	0.305	-171	23810	0.310	-173	23040
6	0.282	-275	10930	0.281	-275	11390
8	0.154	-248	34190	0.150	-248	36880
10	0.035	143	76130	0.034	125	81320

FIG. 1. Interference between two time delay processes due to the change in frame transformation.

FIG. 2. Four coordinate systems  $xyz$ ,  $x'y'z'$ ,  $x''y''z''$ , and  $x'''y'''z'''$  pertaining to the eigenchannels of  $\mathcal{S}^0$ ,  $\mathcal{S}$  or  $\sigma \cdot \mathcal{P}_a$ ,  $\sigma \cdot \mathcal{P}_f$ , and  $\sigma \cdot \mathcal{P}_t$ .

FIG. 3. A diagram showing the spherical polar coordinates of  $\hat{n}_t$  in the  $xyz$  and  $x'y'z'$  coordinate systems. The projection of  $\hat{n}_t$  on the  $x'y'$  plane coincides with  $\hat{n}_f$  except for the length. Note that  $\hat{n}_a$ ,  $\hat{n}_t$ , and  $\hat{n}_f$  lie on the same plane. This diagram shows that the spherical polar coordinates of  $\hat{n}_t$  in two coordinate systems are given by  $(1, \theta_t, -\Delta_{12}^0)$  and  $(1, \theta_f, -\delta_a)$ , respectively.

FIG. 4. The spherical triangle whose vertices are the endpoints of  $\hat{z}$ ,  $\hat{n}_a$ , and  $\hat{n}_t$ .

FIG. 5. The dual spherical triangle corresponding to the spherical triangle of Fig. 4, where the edge angles of the latter becomes the vertex angles of the former and vice versa.

FIG. 6. A diagram showing the geometrical traversal of the vertex P as energy increases from  $-\infty$  to  $\infty$ , the point P traverses from the point A to the opposite point  $-A$  along the great circle.

FIG. 7. Partial delay times  $2\hbar d\delta_{\pm}/d\epsilon_r$  vs.  $\epsilon_r$  are plotted for three different profile indices  $q_r = 0.6, 1$ , and  $5$  with  $\Delta_{12}^0 = \pi/3$ . Graphs for  $2\hbar d\delta_+/d\epsilon_r$  are located more shifted to the left hand side than the corresponding ones for  $2\hbar d\delta_-/d\epsilon_r$ . The values  $0.6$  of  $q_r$  is close to its possible minimum value  $0.577$  ( $=\cot \Delta_{12}^0$ ).

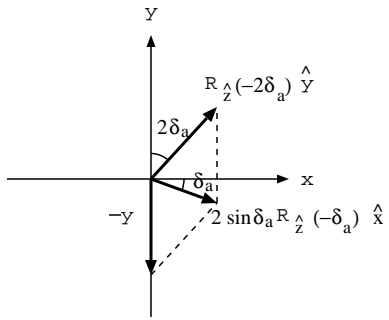


Fig. 1 (lee)

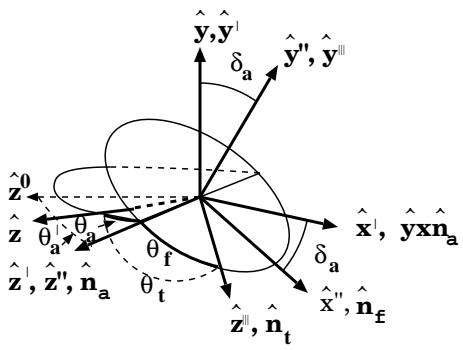


Fig. 2(lee)

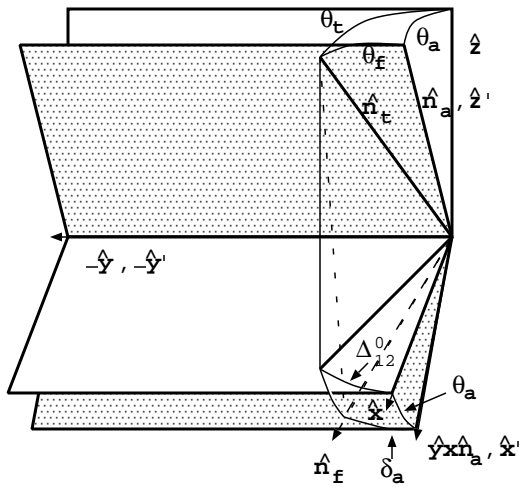


Fig. 3 (lee)

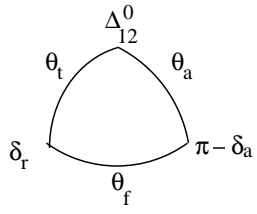


Fig. 4 (lee)

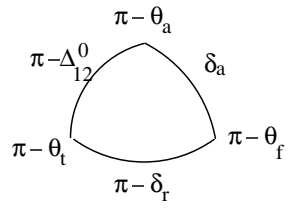


Fig. 5 (lee)

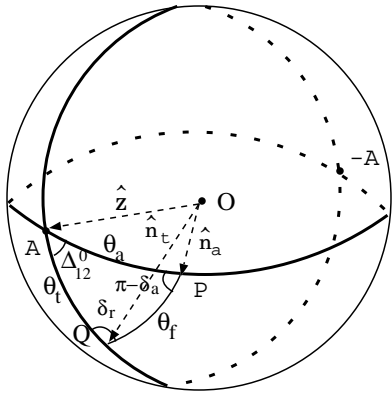


Fig. 6(lee)



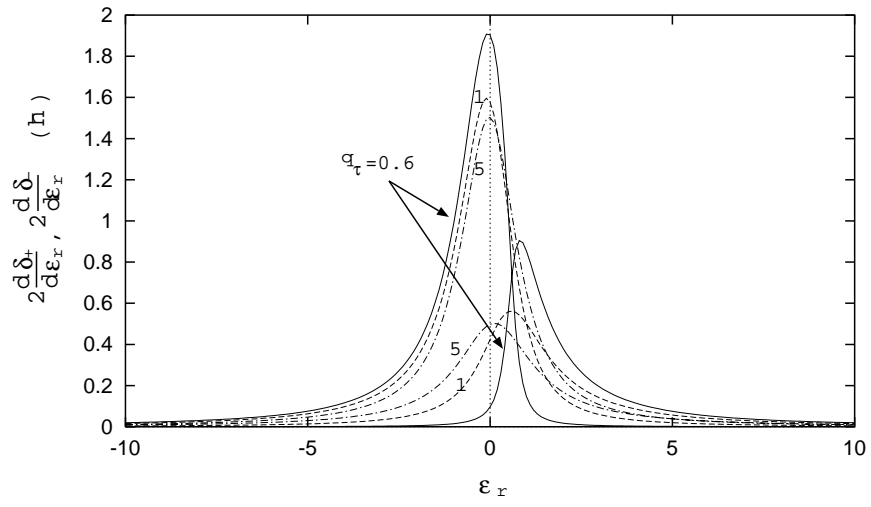


Fig. 7(lee)